This is a preprint, the final version is subject to change, of the American Mineralogist (MSA)
Cite as Authors (Year) Title. American Mineralogist, in press.
(DOI will not work until issue is live.) DOI: http://dx.doi.org/10.2138/am.2013.4275

Revision 1

Remobilization of U and REE and the formation of secondary minerals in oxidized U deposits

Susanne Göb[1], Jan-Erik Gühring[1], Michael Bau[2], and Gregor Markl[1]

[1] Fachbereich Geowissenschaften, Eberhard Karls Universität Tübingen, D-72074 Tübingen, Germany

[2] Earth and Space Science Program, Jacobs University Bremen, D-28759 Bremen, Germany

Abstract

The hydrothermal uranium vein-type deposits of Menzenschwand and Wittichen in the Schwarzwald in south-western Germany have been investigated with regards to their primary and secondary mineralization. Primary magmatic uraninite I from the host granite of Menzenschwand, primary hydrothermal uraninite II and secondary (supergene) uranyl silicates (uranophane and cuprosklodowskite), uranyl phosphates (torbernite and uranocircite) and uranyl arsenates (zeunerite, heinrichite, nováčekite, walpurgite and uranospinite) were analyzed for their REE contents by LA-ICP-MS together with uraninite II samples from other known Schwarzwald uraninite II occurrences for comparison. Water samples were taken from drillings and abandoned mines and were analyzed for their major and trace element composition including U and REE.

The REE patterns of uraninite show significant Eu anomaly variations: negative Eu anomalies are related to granitic host rocks, whereas positive Eu anomalies imply a gneissic REE source. This is in agreement with the observation of Eu anomalies in granite and gneiss derived waters, which display negative and positive Eu anomalies, respectively.

Rare earth element distributions in the secondary uranyl minerals provide information about the sequence of mineral precipitation and the degree of remobilization of U. Ce anomalies (or their absence) imply that uranyl silicates formed during an earlier stage of weathering under more reduced conditions than the uranyl arsenates and phosphates. The REE patterns of the uranyl silicates in Wittichen are similar to those of uraninite II, suggesting a very local redistribution on the mm- to cm-scale. In contrast, the REE patterns of uranyl arsenates and phosphates are different from uraninite II patterns and resemble those of the waters. This shows that the uranyl phosphates and arsenates are formed not only by redistribution of U in the hydrothermal veins but are influenced by waters from the host rock implying that U was probably transported over a greater distance. These conclusions are supported by field observations, where uranyl silicates are often found in the vicinity of uraninite II whereas

uranyl phosphates and arsenates are commonly found on fissures in the host rock.

To explain specific features in the sulfide-rich (pyrite, chalcopyrite) Menzenschwand deposit, we conducted thermodynamic reaction modeling using the PHREEQC computer code. Sulfide oxidation was modeled by reaction of a U-rich water in equilibrium with atmospheric oxygen with FeS_2 and $CuFeS_2$. A water that initially precipitates uranophane gradually evolves to more acidic pH values, thereby reaching torbernite saturation. This is in agreement with observed paragenetic sequences. Ongoing reaction results in a further decrease of pH and in the destabilization of uranophane and torbernite. Since goethite precipitates even at low pH values, these calculations can explain observed pseudomorphs of goethite after both uranophane and torbernite, which are frequently observed at Menzenschwand. If the reaction proceeds and fO_2 in the system is buffered by the surrounding minerals, U^{6+} can be reduced to U^{4+} and uraninite can form and replace pyrite and earlier formed secondary uranium minerals such as ianthinite. Also these textures have been observed. We show that the combination of REE geochemistry, careful paragenetic observations and thermodynamic modelling allows to reconstruct the formation and weathering of uranium deposits in great detail.

Keywords: uranium, rare earth elements, supergene alteration, thermodynamic stability

Introduction

Uranium occurs in nature as U^{4+}, which is the dominant oxidation state under reduced conditions, and as U^{6+}, which predominates in more oxidized environments (Langmuir 1978). U^{4+} has generally low solubilities, whereas U^{6+} is relatively soluble in aqueous fluids as UO_2^{2+} complexes (Murphy and Shock 1999). It is mobilized as phosphate complexes under neutral conditions, whereas it forms carbonate complexes in alkaline waters (Langmuir, 1978) and sulfate complexes in acid drainage (Brugger et al. 2003). Organic ligands can also play an important role (Trenfield et al. 2011). This can lead to high U concentrations and mobility in oxidized waters flowing through uranium-bearing rocks. From these waters, uranyl minerals can precipitate, thereby decreasing the U content of a water (Finch and Murakami 1999; Jerden and Sinha 2003). These minerals can be oxyhydroxides (e.g., schoepite), silicates (e.g., uranophane, sklodowskite, cuprosklodowskite), carbonates, sulfates, arsenates (e.g., zeunerite, uranospinite) or phosphates (e.g., torbernite, uranocircite). Formation of uranyl minerals by replacement reactions is frequently observed (Murakami et al. 1997; Pinto et al. 2012): the oxidation of uraninite commonly leads to the formation of uranyl oxihydroxides first, which are then replaced by uranyl silicates and late uranyl phosphates (Finch and Murakami 1999).

To reduce U concentrations in contaminated groundwater, various remediation methods have been proposed. Since pump and treat methods are expensive and not sufficiently effective (Travis and Doty 1990; Abdelouas et al. 1999 and references therein) recent work put effort in the development of in situ methods. These methods aim to immobilize U by sorption or precipitation. The addition of hydroxyapatite has been shown to facilitate precipitation of uranyl phosphates, which can reduce U concentration in the environment (Arey et al. 1999). Permeable reactive barriers using hydroxyapatite as reactive material were shown to effectively remove U from groundwater (Fuller et al. 2002; Simon et al. 2008). Hence, stability limits and natural paragenetic sequences of various secondary uranyl minerals including phosphates are of increasing interest with regards to the environmental impact of

uranium mining and nuclear-waste disposal.

Since REE (rare earth elements + Y) are known to serve as natural tracers for low-temperature geochemical processes (e.g., Johannesson et al. 1997; Aubert et al. 2004, 2001; Leybourne et al. 2006; Ma et al. 2011), REE distributions of uranium minerals, waters and potential REE sources can give information about mobilization processes. To evaluate the conditions that arise during U deposit weathering and lead to the formation of certain uranyl minerals, we analyzed REE concentrations in a variety of magmatic and hydrothermal (primary) uraninite and supergene (secondary) uranyl minerals as well as natural water samples to reconstruct fluid and element sources as well as mobilization distances and Eh-pH conditions during formation and weathering of uranium deposits. Our analyses of natural samples (both solid and fluid samples) were augmented by thermodynamic calculations using the PHREEQC computer program (Parkhurst and Appelo 1999) to put them into a rigorous thermodynamic framework of interpretation.

Geological background

The U deposits investigated in the present study belong to the hydrothermal vein-type deposits of the Schwarzwald in southwestern Germany. The veins crosscut the granites and gneisses of the Varicscan basement of the Schwarzwald (Kalt et al. 2000) and in parts also the Mesozoic red beds, which non-conformably overlay the crystalline rocks in the northern and eastern Schwarzwald. To the west, the Schwarzwald is bordered by the Eocene Upper Rhine Graben (URG; Schwarz and Henk 2005).

Hydrothermal activity during the last 300 Ma (Pfaff et al. 2009) led to the formation of hydrothermal veins throughout the whole Schwarzwald (Metz et al. 1957; Bliedtner and Martin 1986). These veins are fluorite-barite-quartz-carbonate veins with Cu-Bi, Ag-Bi-Co-Ni-U, Pb-Zn, Fe-Mn and Cu-Pb ores (Metz et al. 1957; Bliedtner and Martin 1986; Staude et al. 2012, 2010, 2009).

Deposits with significant uranium mineralization occur at three localities in the Schwarzwald: Menzenschwand in the southern Schwarzwald, Wittichen in the central Schwarzwald and Müllenbach in the northern Schwarzwald (Fig. 1; Kirchheimer 1951, 1953, 1957; Hauptmann 1976; Zuther 1983; Hofmann 1989). At other localities, U minerals (mainly uraninite II) occur in only small quantities (Fig. 1 and Table 1). Uranium deposits are mostly related to granites, only St. Ulrich and Holderpfad/Sulzburg are hosted by gneisses (Fig. 1).

The uranium deposit of Menzenschwand was mined for uranium until 1991 and produced about 1000t U (Markl and Wolfsried, 2011). It is hosted in the vicinity of the NNW-SSE striking Krunkelbach fault in the Bärhalde granite, which averages 14 ppm U, mostly in magmatic uraninite I (Hofmann 1989). This uraninite I was suggested to be the source for the hydrothermal vein deposit consisting of quartz-barite-fluorite veins with pyrite, uraninite II and hematite (Hofmann 1989). In the north and northwest, the deposit is very close to paragneisses, which were also intersected by drillings east and west of the mineralized NNW-SSE striking fault (Bültemann 1990). In the west and southwest, Paleozoic schists occur in some hundred meters distance from the deposit. The formation of the deposit was dated at 310 Ma (Wendt et al. 1979; Hofmann and Eikenberg 1991; Meshik et al. 2000), but some U from uraninite II was remobilized at about 60 Ma (Wendt et al. 1979; Hofmann and Eikenberg 1991). Oxidation of the deposit led to the formation of secondary uranyl minerals like uranophane, uranocircite and torbernite and U-free minerals like gorceixite and churchite (Hofmann 1989; Göb et al. 2011; Markl and Wolfsried 2011). ^{234}U-^{230}Th ages of secondary uranium minerals date this oxidation event to 250-350 ka (Hofmann and Eikenberg 1991), whereas the lower intercept of U-Pb dating on uranocircite gave an age of 1.7 Ma (Pfaff et al. 2009).

In the hydrothermal barite veins at Wittichen, U occurs in uraninite II together with Co- and Ni-arsenides and native Ag and Bi in an unconformity-related deposit (Staude et al. 2012). Uraninite II formation was dated to 245-235 Ma (Meshik et al. 2000, Leibiger 1955) and 158

Ma (Pfaff et al. 2009). Oxidation products are uranophane, zeunerite and other uranyl arsenates. Wittichen is the type locality for a number of secondary uranium minerals such as meta-kirchheimerite (Walenta, 1958), meta-nováčekite (Walenta, 1958), orthowalpurgite (Krause et al. 1995) and others. In contrast to Menzenschwand, no uranyl phosphates are known to occur at Wittichen (Markl and Slotta 2011).

The Müllenbach deposit in the northern Schwarzwald is hosted by Upper Carboniferous arkoses. Hydrothermal uraninite II occurs together with sulfides, arsenides and hematite (Zuther 1983). At Nussbach, located in the southern part of the Triberg granite, the mineralization resembles the Co-Ni-Bi-As-U type that occurs in Wittichen (Steen 2007). The Hammereisenbach U deposit hosted by the Hochfirst-Eisenbach granite contains uraninite II together with native As in quartz veins (Fritsche and von Pechmann 1985; Steen 2007). Near St. Ulrich and Sulzburg, quartz veins that are hosted by gneisses contain uraninite II associated with pyrite, chalcopyrite, tetraedrite, sphalerite and galena (Schatz and Otto 1989). At Detzeln, uraninite II occurs as earthy crusts on fissures of a porphyry (Falkenstein 2010).

Samples

The present study presents the systematics of REE in different U phases from Menzenschwand in the southern Schwarzwald and Wittichen in the central Schwarzwald. For comparison, uraninite II samples from other localities in the Schwarzwald were analyzed. Table 1 reports an overview of the analyzed samples and their localities.

Samples from Menzenschwand include primary magmatic uraninite I (octahedral crystals; Fig 2a) from the host granite, primary hydrothermal uraninite II and secondary uranyl silicates (uranophane, β-uranophane, cuprosklodowskite), phosphates (torbernite and uranocircite) and arsenates (zeunerite). Hydrothermal uraninite II occurs as botryoidal aggregates in the hydrothermal vein (Fig. 2b). In contrast, the supergene uranyl minerals can be found in vugs in the vein (Fig. 2c and d) but also on fissures in the granitic host rock (Fig. 2e). It is

noteworthy, that uranophane occurs mostly in the vein, close to weathered uraninite II, while uranocircite and torbernite are quite common also on granite fissures further away from uraninite II. The replacement of uranyl minerals by goethite (Fig. 2f) and (more rarely) by uraninite III (Fig. 2g) as well as a replacement of pyrite by uraninite III (Fig. 2h) has been described (Ramdohr, 1963; Hofmann 1989; Markl and Wolfsried 2011). The REE phosphate churchite occurs quite commonly as late precipitation in Menzenschwand (Göb et al. 2011). The uranyl mineral samples from Menzenschwand were identified by X-ray diffraction and electron microprobe analysis in former studies (Hurtig 2007; Markl and Wolfsried 2011).

Samples from Wittichen include primary hydrothermal uraninite II and secondary uranyl silicates (uranophane) and arsenates (zeunerite, heinrichite, nováčekite, walpurgite, uranospinite). Uraninite II occurs in the vicinity of biotite in the host rock or together with calcite or native Bi in the veins (Staude et al. 2012). Uranophane is rather rare and occurs only in the immediate vicinity of (mostly strongly altered) uraninite II, whereas zeunerite and heinrichite are abundant both in vein and in granitic host rock samples. Uranospinite is interpreted to be the youngest uranyl phase, as it occurs as crusts close to uraninite II, formed after mining had ceased.

Besides the primary and secondary uranium mineral samples from the U deposits Menzenschwand and Wittichen, hydrothermal uraninite II samples from other localities in granitic and gneissic host rocks of the Schwarzwald were analyzed (Table 1 and Fig. 1). At these localities uraninite is less abundant than at Menzenschwand and Wittichen and it occurs as botryoidal masses in the ore zone. Uraninite from the Müllenbach deposit forms porous aggregates intergrown with quartz and clay minerals.

In addition to the mineral samples, waters from Menzenschwand and Wittichen were sampled. Since the uranyl minerals are interpreted to have formed relatively recently, the modern mine waters are assumed to reflect the mineral-forming waters. Water samples were analyzed for their major and trace element content (including U and REE). In

Menzenschwand, waters originating from two drillings into and close to the abandoned mine (used as spa waters since 2005) could be sampled. One of them is a fluorine-bearing water (sample MenzF2), the other one contains Rn (information Radon Revital Spa at Menzenschwand; sample MenzRn1). A third sample was taken from a runoff of the abandoned mine (sample MenzGru3). In the Wittichen area, water samples from abandoned mines with Co-Ni-As-Bi-U mineralization and Cu-Bi mineralization were taken (for information about localities, vein types and mineralization see Table 2).

Methods

LA-ICP-MS

Trace element concentrations in uraninite and uranyl minerals were determined by LA-ICP-MS at the GeoZentrum Nordbayern of the University of Erlangen-Nürnberg using a UP193FX New Wave Research laser with a wavelength of 193 nm connected to an Agilent 7500i ICP-MS. He and Ar were used as carrier gas. Ablation was carried out at laser energy densities of 2.88 J/cm^2 with a spot size of 25 μm and a repetition rate of 15 Hz. For data reduction, the software GLITTER 3.0 (Macquarie Research Ltd., 2000) was used with NIST 610 as external standard and $^{2\,38}$U as internal standard. Integration time was set to 5 ms for all elements except for ^{238}U for which 10 ms were chosen. Standard values were taken from Pearce et al. (1997). Precision and reproducibility were monitored by ablation of NIST 612 as an unknown sample. Standard deviations (1σ) for REE are 3-4% for uraninite analyses, ~5% for uranophane and, due to low REE concentrations, up to 30% in uranyl phosphates and arsenates. Since BaO interferes with Eu during ICP-MS analyses, Eu concentrations in minerals with high Ba contents (uranocircite, heinrichite) are highly uncertain.

All samples were normalized to the ideal U content of the stoichiometric mineral formula. This might introduce a small error concerning the absolute element concentrations, but relative concentrations (e.g., REE patterns or element ratios) are not affected. The results of

all LA-ICP-MS analyses can be found in the electronic supplement, selected analyses are listed in Table 3 and 4.

Water samples

Water samples were taken in acid-cleaned 1L PE bottles. Temperature, conductivity and pH were determined at the sampling site, alkalinity was determined by titration directly after sampling in the field. For further analysis, water samples were filtered through a 0.2 µm cellulose acetate filter and acidified to pH 2 to prevent precipitation. Samples were filtered and acidified either directly in the field or upon return to the laboratory, directly after sampling. Major anions and cations were analyzed by ion chromatography using a Dionex ICS1000 System with CS12-A (cations) and AS9-HC (anions) ion chromatography columns. For REE analyses, REE were pre-concentrated following the method of Bau and Dulski (1996). The pre-concentration of REE was done at the Fachbereich Geowissenschaften, Universität Tübingen, ICP-MS measurements were performed at the Jacobs University Bremen. Details about ICP-MS measurement conditions and interferences can be found in Alexander (2008). Precision of measurement is, based on repeated standard analyses, is less than 10%. Due to the separation of REE from matrix elements, analytical artifacts resulting from analyte interferences during ICP-MS analysis are negligible. Further trace element concentrations were determined by ICP-MS analysis of acidified sample aliquots at the Karlsruhe Institute of Technology using a high-resolution (HR-)ICP-MS axiom (VG Elemental). Precision for trace elements is better than 3%; for Si, Al and Fe, precision is better 6%.

Results

Magmatic uraninite I

Primary magmatic uraninite I (sample M34/1) from the Bärhalde granite contains 4000 to

6500 ppm ∑REE. Normalized to Post Archean Australian Shale (PAAS, McLennan 1989), a strongly negative Eu anomaly ($Eu/Eu^*=Eu_{norm}/(Sm_{norm}\cdot Gd_{norm})^{0.5}$=0.01 to 0.03) and a slightly positive Ce anomaly ($Ce/Ce^*=Ce_{norm}/(La_{norm}\cdot Pr_{norm})^{0.5}$=1.36 to 1.60) are apparent. Light rare earth elements (LREE) are depleted (La_{norm}/Gd_{norm}= 0.004 to 0.007) compared to heavy rare earth elements (HREE; Gd_{norm}/Lu_{norm}= 1.02 to 1.34).

Hydrothermal uraninite II

Uraninite II from the hydrothermal veins contains REE in variable concentrations. In Wittichen, ∑REE are between 23.000 and 64.000 ppm. In Menzenschwand, REE contents are lower and are in the range from 600 to 10.000 ppm. Uraninite II samples from the other localities have ∑REE between 11.000 and 37.000 ppm, only the samples from Triberg and Müllenbach have ~800 and ~6000 ppm ∑REE, respectively (Table 3). Ce anomalies in all uraninite II samples range from Ce/Ce*=0.9 to 1.9 (Fig. 3). Eu anomalies vary (Fig. 4), in the samples from St. Ulrich they are positive in the range Eu/Eu*=4.5 to 5.0, the samples from Holderpfad range from 2.6 to 3.4. Eu anomalies in the Menzenschwand uraninite II are slightly positive ranging from Eu/Eu*=1.04 to 2.7. Only one sample has a negative Eu anomaly of 0.4. The Wittichen uraninite II samples have slightly negative Eu anomalies with Eu/Eu* values of 0.66 to 0.93. Eu anomalies at other localities range from 0.12 to 1.0. Uraninite II samples are all relatively depleted in LREE relative to HREE (Fig. 4). La_{norm}/Gd_{norm} ratios are between 0.25 and 0.02 for the Menzenschwand samples. The Wittichen uraninite II samples are more strongly depleted in LREE having La_{norm}/Gd_{norm} ratios between 0.0007 and 0.004. All other uraninite II samples have La_{norm}/Gd_{norm} ratios between 0.00007 and 0.34. Y/Ho ratios in uraninite II from Menzenschwand vary from 17.1 to 63.0, in the Wittichen uraninite II Y/Ho ratios range from 10.9 to 16.1.

Uranyl silicates (uranophane, β-uranophane and cuprosklodowskite)

The REE concentrations in uranophane, β-uranophane and cuprosklodowskite are in the range of ∑REE=100 to 1300 ppm (Table 4). Most uranyl silicate samples from Menzenschwand and Wittichen do not show significant Ce anomalies (Ce/Ce*=0.9 to 1.1; Fig. 5). Only two samples have negative Ce anomalies (0.4 to 0.6). Eu anomalies in Wittichen are slightly negative (0.81 to 0.96), whereas they are positive in Menzenschwand (1.2 to 2.1). Uranyl silicate samples are depleted in LREE (La_{norm}/Gd_{norm}=0.04 to 0.002). The Menzenschwand uranyl silicate samples are also depleted in HREE (Gd_{norm}/Lu_{norm}= 4.3 to 43.9). Y/Ho ratios in uranyl silicates range from 8.8 to 27.7 in the Menzenschwand samples and from 18.7 to 24.5 in the Wittichen samples.

Uranyl phosphates and arsenates

The uranyl phosphates and arsenates (Table 4) contain REE in the range from 0.1 to 40 ppm (with one exception; SG256). Ce anomalies are not present or slightly positive (Ce/Ce*=1.00 to 1.3) in four analyses. All other analyses (n=80) showed negative Ce anomalies between 0.02 and 0.9 (Fig. 5). The LREE are depleted relatively to HREE (La_{norm}/Gd_{norm} = 0.002 to 1.7 and Gd_{norm}/Lu_{norm} = 0.1 to 5.0). Y/Ho ratios range from 11.7 to 97.9 in the secondary uranyl arsenates from Wittichen and from 14.2 to 186.1 in the uranyl phosphates and arsenates in Menzenschwand.

Water samples

The three water samples taken from Menzenschwand are all Ca-HCO_3-dominant waters (Table 2). The pH values of the waters are near neutral between 6.6 (MenzF2) and 7.3 (MenzRn1). Sample MenzF2 and MenzGru3 have higher F and Ba contents than sample MenzRn1. The total REE concentrations in the three samples are $7.11 \cdot 10^{-4}$ ppm (MenzRn1), $1.04 \cdot 10^{-4}$ ppm (MenzF2) and $1.80 \cdot 10^{-4}$ ppm (MenzGru3). Ce anomalies are negative for the three samples (Ce/Ce*=0.13 for MenzRn1; 0.56 for MenzF2 and 0.50 for MenzGru3). Eu

297 anomalies are slightly positive (Eu/Eu*=1.1 for MenzRn1; 1.2 for MenzF2 and 1.21 for
298 MenzGru3; Fig. 5). The Wittichen water samples are Ca-HCO_3-dominant and have pH values
299 between 6.3 and 8.3. The total REE concentrations vary from $1.58 \cdot 10^{-5}$ to $1.88 \cdot 10^{-3}$ ppm. Ce
300 and Eu anomalies are negative in all samples where anomalies could be determined
301 (Ce/Ce*=0.06 to 0.6 and Eu/Eu*=0.2 to 0.9). LREE are depleted relative to HREE
302 (La_{norm}/Gd_{norm} = 0.04 to 0.2 and Gd_{norm}/Lu_{norm} = 0.6 to 3.0). Y/Ho ratios in the
303 Menzenschwand waters range from 38.6 to 68.74 and from 25.5 to 60.1 in the Wittichen
304 samples.
305
306 **Discussion**
307 **REE in hydrothermal uraninite II**
308 REE patterns in hydrothermal uraninite II from the Schwarzwald show striking differences
309 especially in their Eu anomalies (Fig. 4). The granite-hosted samples from Hammereisenbach
310 and Detzeln have negative Eu anomalies (Eu/Eu*=0.12-0.17). In contrast, uraninite II samples
311 from Holderpfad and St. Ulrich, which are hosted by gneisses, show positive Eu anomalies
312 (Eu/Eu*=2.44-5.00). The feature of positive Eu anomalies related to gneisses and negative
313 Eu anomalies associated to granites has already been observed by Schwinn and Markl (2005).
314 They found that hydrothermal fluorite from gneisses has positive Eu anomalies whereas
315 fluorite from granite displays no or negative Eu anomalies. Leachates from laboratory
316 experiments as well as aquifer waters from gneisses and granites from the Schwarzwald also
317 display positive and negative Eu anomalies, respectively (Möller et al. 1997). Hence, based on
318 the assumption that REE are derived from either a gneiss or granite, Eu anomalies can be used
319 to trace the origin of REE (assuming that REE mobilization and transport occurred in the
320 same physico-chemical environment). Uraninite II from Wittichen, which is hosted by
321 granites, has only slightly negative Eu anomalies (Fig. 4). Since the hydrothermal veins in the
322 Wittichen area are unconformably related and close to a gneissic lens, an influence from the

sediments or the gneiss is likely and explains varying Eu anomalies. The only uraninite II sample hosted by sediments is from the Müllenbach deposit. Its negative Eu anomaly (Eu/Eu*= 0.58) results from the adjacent granite or the host sediment, which is an arkose that formed from the eroded granite.

Sources of REE and U: Uraninite II formation

For the hydrothermal U deposit of Menzenschwand, the genetic model proposed by Hofmann (1989) involves an oxidized, meteoric, U-rich surface fluid and a reduced, ascending hydrothermal fluid. Interaction of both fluids led to precipitation of uraninite II. The U source was suggested to be the surrounding granite, which contains 14 ppm U as magmatic uraninite I in fresh samples, whereas the slightly altered granite contains less U compared to the fresh rock (Hofmann 1989), which suggests that U was leached from the granite. An origin of U from the adjacent paragneisses or schists was considered unlikely by Hofmann (1989), since U concentrations in these rocks are much lower (between 1.5 and 6.6 ppm; Hofmann 1989). Bültemann (1990) showed that the granite is depleted in U close to the U deposit, which suggests mobilization of U from the granite. However, our data show that for the REE, the gneisses have to be considered as a possible source. The magmatic uraninite I (Eu/Eu*= 0.01 to 0.03) as well as the granitic host rock (Eu/Eu*=0.16; Emmermann et al. 1975) show distinctly negative Eu anomalies, while the hydrothermal uraninite II does not. Although uraninite I contains relatively high REE concentrations (∑REE=4000 to 6500 ppm), it is unlikely that the REE in uraninite II originate from uraninite I, because it contributes only about 0.2% to the REE budget of the granite (based on the assumption that all U in the granite occurs as uraninite I, containing 5000 ppm ∑REE and a total REE content of 40 ppm of the whole rock granite). Apatite, which can contain REE even in the low % range might be a possible REE source. However, since apatite from granites and gneisses in the Schwarzwald has negative Eu anomalies (Puchelt and Emmerman 1976; Kizler 2012) and apatite is

relatively resistant with respect to alteration in neutral pH fluids, it seems unlikely that REE in uraninite II originate mainly from apatite. Since positive Eu anomalies in waters from the Schwarzwald can often be related to gneisses and negative Eu anomalies to granites (Möller et al. 1997; Schwinn and Markl 2005; Göb et al. 2011), an origin of REE from the adjacent gneisses, which crop out in the immediate vicinity of the deposit (less than 400 m), seems likely. Hofmann (1989) suggested that REE were probably mobilized from the gneisses and metasediments, because REE concentrations in gneisses and other metasediments are higher than in the granite. If REE from the gneisses are mobilized by the reducing fluid, and U from the granite is mobilized by oxidized surface water, uraninite II that precipitates by mixing of both waters contains U and REE from different sources. This would be in contrast to other studies, which suggested that U and REE are transported together in solution (McLennan and Taylor 1979).

If REE in Menzenschwand were transported in reducing fluids originating from the adjacent gneisses it seems likely that these fluids also transported reduced sulfur, which precipitated sulfides like pyrite. This would explain the abundant occurrence of sulfides in Menzenschwand, whereas they are lacking in Wittichen. The difference between both deposits is consequently reflected also in their secondary mineralization.

Remobilization of REE and U: supergene uranyl mineral formation

Major elements required for the formation of uranyl minerals originate mostly from the ore and gangue minerals in the veins (As, Cu, Bi, Ba, Si) and to a lesser extent also from the host rocks (K, Si, Ca, Mg, P). Since there are no primary phosphate minerals in the veins, P must have been introduced from the host-rock (apatite) or from the surface (decaying organic matter). For the REE, there are different sources that have to be considered. REE could either originate from minerals of the hydrothermal veins (uraninite II, different fluorite generations) or from the host rock (uraninite I, apatite, micas…). Figure 6 provides a schematic overview

375 of the possible REE sources including their REE content and their abundances.

376 Besides the possible sources of the elements, the nature of the mineral-forming fluids has to
377 be considered as well. The secondary uranyl minerals have been dated to 250 to 340 ka
378 (uranophane and different uranyl phosphates; Hofmann 1989) and 1.7 Ma (uranocircite, Pfaff
379 et al. 2009). Since there were no significant geological changes in the area around the
380 Menzenschwand deposit in the time between the uranyl mineral formation and today, it can be
381 assumed that today's waters are similar to those that formed the uranyl minerals and that the
382 formation of these minerals continues until today (indeed, secondary uranyl minerals formed
383 during mining on the walls of the adits). However, the water chemistry may depend on stream
384 velocities, residence times and influence from the atmosphere.

385 Upon remobilization, REE concentrations in U-bearing minerals change: In uranophane,
386 concentrations are lower than in uraninite II. In the uranyl phosphates and arsenates they are
387 again lower than in the uranophane samples (Fig. 5). This is in contrast to the occurrence of
388 uranyl phosphates at the natural fission reactor at Bangombé (Gabon), where uranyl
389 phosphates contain high amounts of REE, and lanthanides and actinides are both immobilized
390 by precipitation of these minerals (Stille et al. 2003).

391 Besides the changing REE concentrations in primary and secondary uranium minerals, the
392 REE patterns of the various sample types vary between the magmatic uraninite I and the
393 hydrothermal uraninite II and also between the uranyl silicates and the uranyl
394 phosphates/arsenates. To quantify differences between REE patterns, La_{norm}/Gd_{norm} and
395 Gd_{norm}/Lu_{norm} ratios are used to record the steepness of LREE and HREE patterns. In
396 Menzenschwand, uraninite II samples have similar La_{norm}/Gd_{norm} and Gd_{norm}/Lu_{norm} ratios as
397 fluorite and a similar observation can be made for Wittichen, where uraninite II has ratios
398 similar to those observed in fluorite I and III (Fig. 7). If we assume that REE patterns in
399 fluorite reflect the REE pattern of the mineral-precipitating hydrothermal fluid (Schwinn and
400 Markl 2005) this seems to hold true for uraninite II as well.

On the other hand, REE patterns in the supergene minerals may differ vastly from the hydrothermal minerals (Fig. 7). Whereas the REE pattern of the uranophane samples in Wittichen are very similar to those of uraninite II, the uranophane samples from Menzenschwand have very different REE patterns, being depleted in LREE and HREE relative to MREE. The REE patterns of uranyl phosphates and arsenates at both localities are similar to those of the waters flowing through the mines (Fig. 5 and 7).

Since REE mobilization depends on many factors, the REE systematics of Menzenschwand and Wittichen are discussed separately. In Wittichen, the primary hydrothermal mineralogy besides uraninite II consists of mostly arsenides (skutterudite, safflorite) and native elements (bismuth, silver, arsenic) and only very subordinately sulfides (emplectite, wittichenite and no pyrite; Staude et al. 2012). Barite is by far the most important gangue mineral. Uranophane occurrences are rare and only observed in direct vicinity (up to mm away) of uraninite II. Similar REE patterns in both minerals imply, that U and REE in uranophane were not transported over a large distance but precipitated at the site of uraninite II dissolution. The REE concentrations of the uranyl arsenates in Wittichen are very low, although the REE concentrations in uraninite II are very high (up to 3 wt%). Upon alteration of uraninite II, U seems to be mobilized, transported and precipitated in uranyl minerals, while the REE are not. Although Wittichen is a locality well-known for its wealth of (partially rare) secondary minerals (Walenta 1972, 1992; Markl and Slotta 2011), there are no distinct REE minerals amongst them (Göb et al. 2011). Hence, although uraninite II with extremely high REE contents is dissolved, the REE are not mobilized. Leibiger (1955) analyzed a batch of fresh uraninite II samples from the Sophia mine and an earthy batch of decomposed U ore from the Anton mine (both in the Wittichen area) for their U and REE contents. He found that the alteration of the U ore lead to a loss of about 9/10 of its U content but the REE content was not affected. A similar observation was made by Walenta (1992), who described a yellowish, earthy matter with enrichments of Y, Gd, Dy, U, Ba, Fe, As and P as relicts after uraninite II

alteration. The U ore as well as the altered remains of the U ore are much more enriched in HREE (Leibiger, 1955) than the uranyl minerals and the water samples from the mines (Fig. 5). Some water samples with high concentrations of REE show REE patterns less depleted in LREE than uraniniter II. Hence, it can be assumed that REE in the waters do not originate from uraninite II but from the host-rock and that high REE contents in the waters are not related to uraninite II dissolution.

Since fluorite and carbonates, which during dissolution might be a REE source for water (Göb et al. 2011), are quite rare in Wittichen, and REE from uraninite II are not mobilized, it seems reasonable that the REE in the mine waters (which also are the waters responsible for secondary mineral formation) are mostly derived from the host rock. Comparing all water analyses from Wittichen shows that, although some water samples were taken from Cu mineralizations in barite veins without U mineralization (Table 2 and Fig. 5), all REE patterns are similar. These observations support the idea that REE patterns in the waters reflect fluid-rock interactions with the host rocks rather than dissolution reactions in the veins (see also Göb et al. 2011).

In Menzenschwand, the general mineralogy differs from that in Wittichen in that the Menzenschwand U mineralization is accompanied by abundant fluorite, hematite and sulfides, particularly large amounts of pyrite. Consequently, also the secondary mineral assemblages of both deposits differ. Whereas the abundance of As in Wittichen leads to the formation of uranyl arsenates and the absence of phosphates, phosphates are at least as abundant as arsenates in Menzenschwand. Comparing the water analyses from Wittichen and Menzenschwand (Table 2), however, shows that phosphate concentrations in the Wittichen waters are much higher than in the Menzenschwand waters; arsenic concentrations are higher in only some of the Wittichen waters. This suggests that phosphate in the analyzed samples is effectively removed from the Menzenschwand waters, most probably by precipitation of phosphates. This hypothesis is supported by the fact that besides uranyl phosphates also other

453 phosphates are common at Menzenschwand, namely the REE phosphate churchite and the Ba-
454 Al phosphate gorceixite (Hofmann 1989; Göb et al. 2011; Markl & Wolfsried 2011).
455 Although the formation ages of the different uranyl minerals seem to be similar (textures do
456 not allow to differentiate uniquely; Hofmann 1989; Pfaff et al. 2009; Markl and Wolfsried
457 2011), the REE distributions of uranyl silicates and phosphates differ significantly from each
458 other. The uranyl silicates are depleted in HREE (Fig. 5) and have REE patterns very different
459 from uraninite II (Fig. 7). If this was a crystal-chemical effect, it should have been observed in
460 the Wittichen uranophane as well. As this is not the case, the REE in the Menzenschwand
461 uranyl silicates do either originate from another source, or REE patterns are modified during
462 transport and precipitation due to different solution-complex stabilities. Since the modern
463 waters flowing through the mine are very fluoride-rich, REE fluoride complexes were
464 probably important during fluid transport. Fluoride complexes with $HREE^{3+}$ are more stable
465 than those with $LREE^{3+}$ (Bau and Dulski 1995; Luo and Millero 2004), which can lead to a
466 depletion of HREE in a precipitating mineral if fluoride activity in the fluid is not lowered.
467 This process might explain the depletion of HREE in the uranyl silicates in Menzenschwand.
468 The negative Y anomaly in the uranophane (Fig. 5) samples supports this hypothesis. If a
469 fluoride-rich water without Y anomaly precipitates F-free minerals, the Y-fluoride complex,
470 which is relatively more stable compared to the REE-fluoride complexes (Luo and Millero
471 2004) will stabilize Y in solution and precipitating minerals can show negative Y anomalies.
472 This is consistent with PHREEQC calculations (for information about modeling conditions
473 see next section), which show that during reaction with sulfides, fluorine is another important
474 complexing agent, although Y is mainly complexed by carbonate (Fig. 8; using data from
475 Spahiu and Bruno, 1995). Calculations including La, Gd and Lu using data from Millero
476 (1992) show that for La (LREE) the fluorine complexes are less important than for Gd
477 (MREE) and that for La (HREE) and especially Y fluorine is an important complexing agent.
478 Since fluorite is not abundant in Wittichen, transport of REE^{3+} as fluoride complexes is

probably less important than at Menzenschwand, and the REE patterns of the uranophane samples are not depleted in HREE.

For the secondary uranyl phosphates and arsenates from Menzenschwand, the same observations as for the Wittichen uranyl arsenates apply. Their REE patterns reflect those of the host-rock derived waters (Fig. 7), which suggests an input from the host rock. However, since fluorite from the vein has a REE pattern similar to those observed in the uranyl phosphates and arsenates, an influence from the vein is also possible.

Modeling of U deposit alteration

To understand the processes that lead to the formation of secondary minerals in a uranium deposit, calculations using the PHREEQC computer program (Parkhurst and Appelo 1999) were performed using the wateq4f database (detailed information about input data and results can be found in the electronic supplement). Since there exist different thermodynamic data for uranyl minerals in the literature and the databases of various computer programs are not consistent with each other, different log K values for uranophane, torbernite and zeunerite were compared (Table 5). For the calculations, data from Pérez et al. (2000) for uranophane were added to the wateq4f database. For torbernite, data from the PHREEQC wateq4f database and from Ilton et al. (2012) were used and compared. As there exist no reliable data on natural uranyl arsenates (Guillaumont et al. 2003), an estimation of a log K value from van Genderen and van der Weijden (1984) for zeunerite and a log K value from solubility experiments for meta-zeunerite (Vochten and Goeminne 1984) were used and compared.

The most striking difference between the various thermodynamic data emerges, when the P/As ratio for the torbernite-zeunerite transition is calculated (Fig. 9). The combination of data from Vochten and Goeminne (1984) for zeunerite and from Ilton et al. (2010) for torbernite is the only data pair to give geochemically reasonable P/As ratios, while the other possible data combinations result in much too low ratios (see Fig. 9). Accordingly, we select

505 those data for use in thermodynamic modeling.

506 The water samples that were taken from the mines are all undersaturated with respect to
507 uranyl minerals. However, by water-mineral interaction, elements needed for secondary
508 uranyl minerals, which are frequently observed in the mines, can be enriched locally and
509 uranyl minerals can precipitate. Therefore, water analysis MenzGru3 (Table 2) was
510 equilibrated with certain amounts of minerals such as schoepite or tenorite to reach higher
511 concentrations of the necessary elements. This process can be assumed to take place locally.

512 The stability of uranium minerals with regards to fO_2 and pH was tested by calculating a
513 water containing U, Si, Fe, Cu and P at varying fO_2 and pH, and uraninite, schoepite,
514 uranophane, torbernite and goethite were precipitated when saturated. Concentrations of
515 elements in the initial water were reached by equilibration of the water analysis MenzGru3
516 (Table 2) with quartz, schoepite, tenorite and hydroxyapatite at a log fO_2 of -0.68 and pH 6.
517 Conditions of this water were then changed for oxygen fugacities from log fO_2=-80 to 0 and
518 pH values from 1 to 13 (using PhreePlot, Kinniburgh and Cooper 2011). Calculations with the
519 same solution but in equilibrium with $Cu_3(AsO_4)_2 \cdot 6H_2O$ instead of tenorite were performed
520 to find the stability range for the Cu-uranyl arsenate zeunerite as analogue to torbernite.

521 If pH and fO_2 of the fluid are varied, various minerals precipitate when oversaturated. These
522 comprise uraninite, schoepite, uranophane, torbernite and goethite as shown in Figure 10. It is
523 obvious that uraninite is only stable under reduced conditions (up to log fO_2=-40 to -50).
524 Under more oxidized conditions (log fO_2>~-50) uranophane is stable under more alkaline
525 conditions than torbernite, which only occurs in a narrow range around pH 6 when using data
526 from the wateq4f database (based on Langmuir 1978). Data from Ilton et al. (2010) indicate a
527 stability of torbernite over a greater pH range from near neutral to acidic pH values. Schoepite
528 is stable under alkaline conditions only. Goethite is stable over a large fO_2 – pH range and at
529 oxidized conditions even at very low pH values. Calculations with arsenate instead of
530 phosphate show that, using data from van Genderen and van der Weijden (1984), the uranyl

arsenate zeunerite is stable in the same range as torbernite. Using the data determined by Vochten and Goeminne (1984) show a stability field of zeunerite over a much greater pH range.

The stability of zeunerite and torbernite is almost independent of pH (Fig. 9). Since As and P are geochemically very similar, their predominant species in aqueous solution is the same at most conditions. Above a pH of 7.2, $HAsO_4^{2-}$ is the predominant As species, whereas below that pH $H_2AsO_4^-$ is dominant. For phosphorous, the change of predominance between HPO_4^{2-} and $H_2PO_4^-$ is at a pH of 7.15. Accordingly, a pH-dependence of zeunerite or torbernite formation only occurs in the narrow range between pH 7.15 and 7.2.

As sulfide oxidation plays an important role in the alteration of the U deposit Menzenschwand, sulfide oxidation was modeled by reaction of an oxidized fluid (water in equilibrium with atmospheric oxygen (O_2[g]), corresponding to 0.268 mmol/L O_2 [aq]) with $CuFeS_2$ and FeS_2 to investigate mineral dissolution and precipitation during this process. As initial water composition, the water analysis MenzGru3 (Table 2) was set in equilibrium with atmospheric fO_2 and fCO_2, quartz and 0.0001 mol hydroxyapatite and 0.0001 mol uraninite. Oversaturated minerals were precipitated. The resulting water was then used to model a system where water in equilibrium with the atmosphere reacts with 7.5 µmol $FeCuS_2$ and 75 µmol FeS_2 ($FeCuS_2$: FeS_2 = 1 : 10 to approximate the natural example; Hofmann 1989) and is, from then on, not in equilibrium with a fixed fO_2 but fO_2 is determined by the dissolution and precipitation of the involved minerals. Uraninite, schoepite, uranophane, torbernite (using data from Ilton et al. 2010) and goethite are precipitated if oversaturated.

At the U deposit Wittichen, ore minerals in the U mineralization are arsenides, and sulfides, which are abundant in Menzenschwand, are rare. Arsenides have a similar effect as sulfides: if they are oxidized, the pH of the fluid decreases. However, since the predominant arsenic species between pH 7.2 and 2.1 is $H_2AsO_4^-$, this effect is weaker than during sulfide oxidation, where SO_4^{2-} is the dominant sulfur species. By modeling a reaction with 70 µmol

of $FeAs_2$, the conditions of arsenate or phosphate formation can be evaluated. As initial solution, the water analysis MenzGru3 was equilibrated with atmospheric fO_2 and fCO_2, quartz, 0.0001 mol of hydroxyapatite and 0.0005 mol of uraninite. Oversaturated minerals were precipitated. During reaction, with the arsenide, fO_2 was determined by dissolution and precipitation of the involved minerals. Uraninite, schoepite, uranophane, zeunerite (using data from Vochten and Goeminne 1984) and goethite are precipitated if oversaturated.

The results of the reaction calculations show that water at atmospheric conditions (log fO_2=-0.68) reacting with quartz, apatite and uraninite precipitates uranophane. If this water, after uranophane precipiation, reacts with $CuFeS_2$ and FeS_2, torbernite precipitates. When the amount of reacted sulfide increases, the pH in the resulting fluid decreases and uranophane and torbernite become unstable while goethite still precipitates (Fig. 11). Further reaction with sulfide leads to a decrease of fO_2, which stabilizes secondary uraninite III. Whereas under near neutral, oxidized conditions U is mainly complexed by phosphate, under reduced conditions the importance of the $U(OH)_4$ complex increases.

Reaction calculations with $FeAs_2$ show that uranophane is only stable if little $FeAs_2$ react and the stable uranyl phase is zeunerite. Torbernite does not occur in this model (Fig. 12). The evolution of pH during the reaction with arsenide is similar to that with sulfides. However, oversaturation of uraninite is only reached in the sulfide reaction simulations. This is in agreement with the observations in Wittichen, where arsenide oxidation is assumed to play a major role and no secondary uraninite III occurs.

Comparison of model and observations from nature

The combination of calculated mineral stabilities with the results of trace element analyses can explain some of the observed mineral textures and provides information about the alteration process.

1. Uranophane samples do not display Ce anomalies whereas uranyl phosphates do (Fig. 5).

583 Although Ce oxidation is a process that is kinetically inhibited, it can be mediated by
584 microbial activity (Moffett 1990). Immobilization of Ce^{4+} by adsorption to mineral surfaces,
585 especially Mn oxides (e.g., Takahashi 2000; Loges et al. 2012), can then lead to a negative Ce
586 anomaly in the fluid and hence in precipitating minerals. Since negative Ce anomalies in
587 surface waters develop quickly (Leybourne et al. 2000) and are commonly observed, it might
588 be presumed, that the water that precipitated the uranyl silicates was not a near-surface water.
589 The uranyl phosphates, in contrast, display negative Ce anomalies and accordingly can be
590 assumed to have precipitated at a shallower depth, closer to the surface than the uranyl
591 silicates. Since Ce^{4+} predominates over Ce^{3+} not only at more oxidizing conditions but also at
592 relatively more alkaline conditions (Möller and Bau, 1993; Akagi and Masuda 1998), one
593 could assume that uranophane formed under more acidic conditions than torbernite. However,
594 as uranophane is not stable under more acidic conditions than torbernite, uranophane must
595 have precipitated at more reduced conditions than the uranyl phosphates.
596 2. At the U deposit Menzenschwand pseudomorphs of goethite after uranophane and
597 torbernite are common (Markl and Wolfsried 2011). Calculations that model the reaction of
598 an oxidized fluid with $FeCuS_2$ and FeS_2 show that during this process, the pH of the fluid
599 decreases and can fall below the stability limits for uranophane and torbernite, which leads to
600 destabilization of the uranyl minerals. In contrast, goethite is stable even under these acidic
601 conditions and precipitates if pyrite oxidizes. Pseudomorphs of goethite after uranophane and
602 torbernite can be the result of this process.
603 3. If the reaction with sulfide proceeds, it can lead to a significant decrease of fO_2 and finally
604 to reduction of U^{6+} to U^{4+} and precipitation of uraninite. The observed pseudomorphs of
605 uraninite III after secondary uranyl minerals (especially ianthinite) or pyrite are nicely
606 explained by this scenario, which would occur if water percolating through the rock gets
607 trapped in a vug and reacts under closed system conditions and low fluid/mineral ratios with
608 the sulfides in direct contact.

609 4. The observations of uranophane and the absence of torbernite in Wittichen agree well with
610 the reaction calculations. As arsenic concentrations are much higher in an arsenide-oxidizing
611 environment compared to an Fe-Cu-sulfide-oxidizing environment, the abundant occurrence
612 of arsenates and the absence of phosphates is expected.
613 5. Comparing the observations from Menzenschwand and Wittichen to other U deposits
614 shows that the alteration processes are similar. At the Koongarra ore deposit in Australia, the
615 primary uraninite from depths 30-100 m is partly altered to uranyl silicates, whereas in the
616 secondary ore deposit (0-30 m deep) weathering of the primary ore lead to the formation of
617 uranyl phosphates (Murakami et al. 1997).
618 Ondruš et al. (2003) made similar observations in the veins of the Jáchymov ore district,
619 Czech Republic, where they found torbernite and uranophane at the outcrop of the secondary
620 zone of the vein, whereas in deeper parts of the vein they found only uranophane and
621 uraninite, and in even deeper parts, in the primary zone, uraninite is the only U mineral
622 observed.
623 Plášil et al. (2006) described uranyl phosphates from near-surface parts in veins of the Horní
624 Slavkov uranium ore district, Czech Republic, and uranyl silicates from depths of 18 and 46
625 m. These observations show that uranophane is usually the uranyl mineral that forms under
626 more reduced conditions. Murakami et al. (1997) observed also that saleeite (uranyl
627 phosphate) replaces sklodowskite (uranyl silicate), and Plášil et al. (2006) described
628 weathered uraninite that was replaced by uranyl silicates, which were later replaced by uranyl
629 phosphates and arsenates. In the last stage of secondary mineralization they observed partial
630 dissolution of uranyl phosphates and precipitation of limonite.
631 The descriptions by Murakami et al. (1997), Ondruš et al. (2003) and Plášil et al. (2006) are
632 very similar to the observations made on the samples from Menzenschwand and Wittichen.
633 The observation that uranyl silicates form in deeper parts of the veins than the uranyl
634 phosphates and arsenates are consistent with the REE patterns of secondary uranyl minerals,

since uranophane and cuprosklodowskite have no Ce anomalies and uranyl phosphates and arsenates have negative Ce anomalies. The dissolution and replacement reactions, which are also observed at other localities, show that the processes modeled here are of general importance during oxidation of a uranium deposit and can explain its evolution.

Since the waters taken from the mines are undersaturated with respect to the uranyl minerals, the formation of frequently found secondary uranyl minerals cannot be the result of precipitation from the analyzed waters. Dall'Aglio et al. (1974), Murakami et al. (1997) and Kaçmaz and Nakoman (2009) have also analyzed waters, which are undersaturated with respect to uranyl phosphates and stated that higher U and P concentrations would be needed for precipitation. However, Murakami et al. (1997) showed that uranyl phosphates can form by local saturation at the interfaces of apatite (as P source) and sklodowskite (U source). Murakami et al. (2005) showed that crystallization of goethite from ferrihydrite releases adsorbed U, P, and Cu or Mg so that nanocrystals of uranyl phosphates formed. In these cases, the uranium required for the formation of uranyl minerals is not only transported in the water but released by minerals that are available at the site of mineral formation.

For the formation of the Wittichen and Menzenschwand uranyl minerals, similar scenarios seem likely. Very local redistribution is certainly the case for the uranophane samples from Wittichen, where uranophane occurs in the vicinity of uraninite II and the REE patterns of both minerals are similar. However, uranyl phosphates and arsenates that are often found in fissures of the host rocks show REE patterns similar to host rock-derived waters, which suggests transport over greater distances (dm to tens of meters). In this case, similar processes as described by Murakami et al. (1997, 2005) might lead to the formation of uranyl phosphates and arsenates. The calculations also show that if after reaction with uraninite and apatite U and phosphate concentrations are high enough, reaction with chalcopyrite can lead to precipitation of Cu-uranyl phosphates.

Taking the considerations from above into account, a chronological and spatial sequence of

661 secondary mineral precipitation can be proposed for the alteration of U deposits. Primary
662 hydrothermal uraninite II becomes unstable if fO_2 increases during oxidation of the deposit
663 and U and trace elements can be released. Uranyl silicates (uranophane and
664 cuprosklodowskite) precipitate under less oxidized conditions than uranyl phosphates and
665 arsenates, which explains the lack of Ce anomalies in the silicates and observed negative Ce
666 anomalies in the phosphates and arsenates. This is consistent with the observations that
667 uranophane occurs in deeper parts of the veins than phosphates (Murakami et al. 1997;
668 Ondruš et al. 2003; Plášil et al. 2006).
669 Dependent on the occurrence and alteration of minerals in a specific deposit, different
670 elements are released, different transport mechanisms take effect and different secondary
671 minerals can form. In Menzenschwand, pyrite is an abundant ore mineral, providing high
672 amounts of Fe and a decrease in pH during oxidation. Abundant fluorite can provide high
673 fluoride concentrations in the water which can complex and transport REE. During a later
674 stage of supergene alteration processes, REE phosphates (churchite, gorceixite) are
675 precipitated (Hofmann 1989; Göb et al. 2011). In contrast, fluorite is not very abundant in
676 Wittichen and the high REE concentrations of uraninite II are probably not mobilized but are
677 concentrated in an amorphous earthy substance in altered uraninite II (Leibiger 1955; Walenta
678 1992) and no discrete REE minerals form (Göb et al. 2011). Since the analyzed water samples
679 from Wittichen and Menzenschwand are undersaturated with respect to uranyl minerals,
680 reaction of these waters with apatite, uraninite, sulfides or arsenides is necessary to precipitate
681 uranyl minerals (Murakami et al. 1997, 2005). Since REE in the waters and in the secondary
682 uranyl phosphates and arsenates are very similar, a host rock-derived fluid must have been
683 involved in the mineral formation.
684

685 **Acknowledgments**

686 We thank Zsolt Berner from the Karlsruher Institut für Technologie for ICP-MS analysis and

Helene Brätz from the GeoZentrum Nordbayern for LA-ICP-MS analysis. Kai Hettmann is thanked for insightful discussions and hints. We thank Martin Herrmann for giving us the possibility to enter the abandoned mines in Wittichen, as well as Mrs. Rupp and Mr. Fritz who gave us the possibility to take water samples in Menzenschwand. Beda Hofmann and Andreas Hauptmann provided sample material, which is greatly acknowledged. We thank Joël Brugger and an anonymous reviewer for their constructive comments that helped to improve the manuscript. This research was supported by the Alfried Krupp Prize for Young University Teachers of the Krupp Foundation to G. Markl.

References

Abdelouas, A., Lutze, W., and Nuttall, H.E. (1999) Uranium Contamination in the subsurface: Characterization and Remediation. In P.C. Burns and R. Finch, Eds., Uranium: Mineralogy, Geochemistry and the Environment, 38, p. 433-473. Reviews in Mineralogy, Mineralogical Society of America, Virginia.

Akagi, T. and Masuda, A. (1998) A simple thermodynamic interpretation of Ce anomaly. Geochemical Journal, 32, 301-314.

Alexander, B.W. (2008) Trace element analyses in geological materials using low resolution inductively coupled plasma mass spectrometry (ICPMS) Technical Report 18, Jacobs University Bremen.

Arey, J.S., Seaman, J.C., and Bertsch, P.M. (1999) Immobilization of uranium in contaminated sediments by hydroxyapatite addition. Environmental Science & Technology, 33, 337-342.

Aubert, D., Stille, P., and Probst, A. (2001) REE fractionation during granite weathering and removal by waters and suspended loads: Sr and Nd isotopic evidence. Geochimica et Cosmochimica Acta, 65, 387-406.

Aubert, D., Probst, A., and Stille, P. (2004) Distribution and origin of major and trace elements (particularly REE, U and Th) into labile and residual phases in an acid soil profile (Vosges Mountains, France). Applied Geochemistry, 19, 899-916.

Ball, J.W. and Nordstrom, D.K. (2001) User's manual for wateq4f, with revised thermodynamic data base and test cases for calculating speciation of major, trace, and redox elements in natural waters. U.S. Geological Survey, Open-File Report 91-183.

Bau, M. and Dulski, P. (1995) Comparative study of yttrium and rare-earth element behaviours in fluorine-rich hydrothermal fluids. Contributions to Mineralogy and Petrology, 119, 213-223.

Bau, M. and Dulski, P. (1996) Anthropogenic origin of positive gadolinium anomalies in river waters. Earth and Planetary Science Letters, 143, 245-255.

Bliedtner, M. and Martin, M. (1986): Erz- und Minerallagerstätten des Mittleren Schwarzwaldes, 782 p. Landesamt für Geologie, Rohstoffe und Bergbau (LGRB), Freiburg i. Br., Germany.

Brugger, J., Burns, P., and Meisser, N. (2003) Contribution to the mineralogy of acid drainage of Uranium minerals: marécottite and the zippeite group. American Mineralogist, 88, 676-685.

Bültemann, W.-D. (1990) Die Uranlagerstätte Krunkelbach bei Menzenschwand, südlicher Schwarzwald. Dissertation Ruprecht-Karls-Universität Heidelberg, Germany, 236 p.

Dall'Aglio, M., Gragnani, R., and Locardi, E. (1974) Geochemical factors controlling the formation of the secondary minerals of uranium. In Formation of Uranium ore deposits p.33-48. International Atomic Energy Agency, Vienna. 748 p.

748

749 Emmermann, R., Daieva, L., and Schneider, J. (1975) Petrologic significance of rare earths
750 distribution in granites. Contributions to Mineralogy and Petrology, 52, 267-283.

751

752 Falkenstein, F. (2010) Ein bislang unbekanntes Mineral- und Fossilvorkommen im Porphyr-
753 Steinbruch bei Detzeln, im südöstlichsten Schwarzwald. Der Aufschluss, 61, 157-174.

754

755 Finch, R. and Murakami, T. (1999) Systematics and paragenesis of uranium minerals. In P.C.
756 Burns and R. Finch, Eds., Uranium: Mineralogy, Geochemistry and the Environment, 38, p.
757 91-179. Reviews in Mineralogy, Mineralogical Society of America, Virginia.

758

759 Fritsche, R. and von Pechmann, E. (1985) Eine Pechblende – gediegen Arsen-Paragenese im
760 Hochfirst-Eisenbachgranit (Schwarzwald). Jahreshefte des geologischen Landesamtes von
761 Baden-Württemberg, 27, 7-15.

762

763 Fuller, C.C., Bargar, J.R., Davis, J.A., and Piana, M.J. (2002) Mechanisms of uranium
764 interactions with hydroxyapatite: Implications for groundwater remediation. Environmental
765 Science & Technology, 36, 158-165.

766

767 Göb, S., Wenzel, T., Bau, M., Jacob, D.E., Loges, A., and Markl, G. (2011) The redistribution
768 of rare-earth elements in secondary minerals of hydrothermal veins, Schwarzwald,
769 southwestern Germany. The Canadian Mineralogist, 49, 1305-1333.

770

771 Guillaumont R., Fanghänel, T., Fuger, J., Grenthe, I., Neck, V., Palmer, D.A., and Rand, M.H.
772 (2003) Update on the chemical thermodynamics of Uranium, Neptunium, Plutonium,
773 Americium and Technetium, 970 p. Elsevier, Amsterdam.

Hauptmann, A. (1976) Zur Petrographie und Radioaktivität des Kirchheimerstollens. 84 p. Diploma Thesis Albert-Ludwigs-Universität Freiburg, Germany.

Hofmann, B. (1989) Genese, Alteration und rezentes Fliess-System der Uranlagerstätte Krunkelbach (Menzenschwand, Südschwarzwald). 195 p. Dissertation, Universität Bern, Switzerland.

Hofmann, B. and Eikenberg, J. (1991) The Krunkelbach Uranium deposit, Schwarzwald, Germany: Correlation of radiometric ages (U-Pb, U-Xe-Kr, K-Ar, ^{230}Th-^{234}U) with mineralogical stages and fluid inclusions. Economic Geology, 86, 1031-1049.

Hurtig, M. (2007) Mineralchemie von Uranglimmern, Uranophan und verwandten Mineralien der ehemaligen Uran-Lagerstätte Krunkelbach bei Menzenschwand, Südschwarzwald. 118 p. Diploma Thesis Eberhard Karls Universität Tübingen, Germany.

Ilton, E.S., Zachara, J.M., Moore, D.A., McKinley, J.P., Eckberg, A.D., Cahill, C.L., and Felmy, A.R. (2010) Dissolution study of metatorbernite: thermodynamic properties and the effect of pH and phosphate. Environmental Science & Technology, 44, 7521-7526.

Jerden, J.L. Jr. and Sinha, A.K. (2003) Phosphate based immobilization of uranium in an oxidizing bedrock aquifer. Applied Geochemistry, 18, 823–843.

Johannesson, K.H., Stetzenbach, K.J., and Hodge, V. (1997) Rare earth elements as geochemical tracers of regional groundwater mixing. Geochimica et Cosmochimica Acta, 61, 3605-3618.

Kaçmaz, H. and Nakoman, M.E. (2009) Hydrochemical characteristics of shallow groundwater in aquifer containing uranyl phosphate minerals, in the Köprübaşı (Manisa) area, Turkey. Environmental Earth Sciences, 59, 449–457.

Kalt, A., Altherr, R., and Hanel, M. (2000): The Variscan basement of the Schwarzwald. Beiheft Europäisches Jahrbuch für Mineralogie, 12, 1-43.

Kinniburgh, D.G. and Cooper, D.M. (2011) PhreePlot - Creating graphical output with PHREEQC. http://www.phreeplot.org.

Kirchheimer, F. (1951) Die Uranerzvorkommen im mittleren Schwarzwald. Mitteilungsblatt der badischen geologischen Landesanstalt, 1-47.

Kirchheimer, F. (1953) Weitere Untersuchungen über das Vorkommen von Uran im Schwarzwald. Abhandlungen des geologischen Landesamtes Baden-Württemberg, 1, 1-60.

Kirchheimer, F. (1957) Bericht über das Vorkommen von Uran im Schwarzwald. Abhandlungen des Geologischen Landesamtes von Baden-Württemberg, 2, 1-127.

Kizler, C. (2012) Selten-Erd-Element-Systematik alterierter Nebengesteine hydrothermaler Erzlagerstätten im Schwarzwald. BSc Thesis, Universität Tübingen.

Krause, W., Effenberger, H., and Brandstätter, F. (1995) Orthowalpurgite, $(UO_2)Bi_4O_4(AsO_4)_2{\cdot}2H_2O$, a new mineral from the Black Forest, Germany. European Journal of Mineralogy, 7, 1313-1324.

826

827 Langmuir, D. (1978) Uranium solution-mineral equilibria at low temperatures with
828 applications to sedimentary ore deposits. Geochimica et Cosmochimica Acta, 42, 547-569.

829

830 Leibiger, H. (1955) Beiträge zur Methodik der Gehaltsbestimmung von Uran und Blei in
831 Uranpecherzen zum Zweck der altersbestimmung und Beiträge zur analytischen Chemie des
832 Urans im allgemeinen. Untersuchungen über das Vorkommen von seltenen Erden und
833 Thorium in den Uran-Kobalt-Erzen des mittleren Schwarzwalds. Erfahrungen und
834 Untersuchungen über die Trennung und Bestimmung von Blei und Wismut mittels Thionalid.
835 Dissertation, Albert-Ludwigs-Universität zu Freiburg im Breisgau.

836

837 Leybourne, M.I., Goodfellow, W.D., Boyle, D.R., and Hall, G.M. (2000) Rapid development
838 of negative Ce anomalies in surface waters and contrasting REE patterns in groundwaters
839 associated with Zn±Pb massive sulphide deposits. Applied Geochemistry, 15, 695-723.

840

841 Leybourne, M.I,, Peter, J.M., Layton-Matthews, D., Volesky, J., and Boyle, D.R. (2006)
842 Mobility and fractionation of rare earth elements during weathering and gossan formation and
843 chemical modification of massive sulfide gossan. Geochimica et Cosmochimica Acta, 70,
844 1097-1112.

845

846 Loges, A., Wagner, T., Barth, M., Bau, M., Göb, S., and Markl, G. (2012) Negative Ce
847 nomalies in Mn oxides: The role of Ce^{4+} mobility during water–mineral interaction.
848 Geochimica et Cosmochimica Acta, 86, 296–317.

849

850 Luo, Y. and Millero, F.J. (2004) Effects of temperature and ionic strength on the stabilities of
851 the first and second fluoride complexes of yttrium and the rare earth elements. Geochimica et

852 Cosmochimica Acta 68, 4301-4308.

853

854 Ma, L., Jin, L., and Brantley, S.L. (2011) How mineralogy and slope aspect affect REE
855 release and fractionation during shale weathering in the Susquehanna/Shale Hills Critical
856 Zone Observatory. Chemical Geology, 290, 31-49.

857

858 Magalhães, M.C.F. and Pedrosa de Jesus, J.D. (1985) The chemistry of uranium dispersion in
859 groundwaters at the Pinhal do Souto mine, Portugal. Inorganica Chimica Acta, 109, 71-78.

860

861 Markl, G. and Slotta, C. (2011) Die Uranmineralien des Lagerstättenreviers Wittichen im
862 mittleren Schwarzwald. Lapis, 36, 25-37.

863

864 Markl, G. and Wolfsried, S. (2011) Das Uran von Menzenschwand 143 p. Christian Weise
865 Verlag München.

866

867 McLennan, S. M. (1989). Rare earth elements in sedimentary rocks: influence of provenance
868 and sedimentary processes. In B.R. Lipin and G.A. McKay, Eds., Geochemistry and
869 Mineralogy of Rare Earth Elements, 21, p. 169-200. Reviews in Mineralogy, Mineralogical
870 Society of America, Virginia.

871

872 McLennan, S.M. and Taylor, S.R. (1979) Rare earth element mobility associated with
873 uranium mineralisation. Nature, 282, 247-250.

874

875 Meshik, A.P., Lippolt, H.J., Dymkov, and Yu, M. (2000) Xenon geochronology of
876 Schwarzwald pitchblendes. Mineralium Deposita, 35, 190-205).

877

878 Metz, R., Richter, M., and Schürenberg, H. (1957) Die Blei-Zink-Erzgänge des
879 Schwarzwaldes, 277 p. Beihefte zum Geologischen Jahresbuch, 29. Hannover, Germany.
880
881 Millero, F.J. (1992) Stability constants for the formation of rare earth inorganic complexes as
882 a function of ionic strength. Geochimica et Cosmochimica Acta, 56, 3123-3132.
883
884 Moffett, J.W. (1990) Microbially mediated cerium oxidation in sea water. Nature, 345, 421-
885 423.
886
887 Möller, P. and Bau, M. (1993) Rare-earth patterns with positive cerium anomaly in alkaline
888 waters from Lake Van, Turkey. Earth and Planetary Science Letters, 117, 671–676.
889
890 Möller, P., Maus, H., and Gundlach, H. (1982) Die Entwicklung von
891 Flußspatmineralisationen im Bereich des Schwarzwaldes. Jahreshefte des geologischen
892 Landesamtes in Baden-Württemberg, 24, 35-70.
893
894 Möller, P., Stober, I., and Dulski, P. (1997) Seltenerdelement-, Yttrium-Gehalte und
895 Bleiisotope in Thermal- und Mineralwässern des Schwarzwaldes. Grundwasser – Zeitschrift
896 der Fachsektion Hydrogeologie, 3/97, 118-132.
897
898 Murakami, T., Ohnuki, T., Isobe, H., and Sato, T. (1997) Mobility of uranium during
899 weathering. American Mineralogist, 82, 888-899.
900
901 Murakami, T., Sato, T., Ohnuki, T., and Isobe, H. (2005) Field evidence for uranium
902 nanocrystallization and its implications for uranium transport. Chemical Geology, 221, 117-
903 126.

Murphy, W.M. and Shock, E.L. (1999) Environmental aqueous geochemistry of actinides. In P.C. Burns and R. Finch, Eds., Uranium: Mineralogy, Geochemistry and the Environment, 38, p.221-253. Reviews in Mineralogy, Mineralogical Society of America, Virginia.

Nguyen, S.N., Silva, R.S., Weed, H.C. and Andrews, J.E. Jr. (1992) Standard Gibbs free energies of formation at the temperature 303.15 K of four uranyl silicates: soddyite, uranophane, sodium boltwoodite, and sodium weeksite. The Journal of Chemical Thermodynamics, 24, 359-376.

Ondruš, P., Veselovský, F., Gabašová, A., Drábek, M., Dobeš, P., Malý, K., Hloušek, J., and Sejkora, J. (2003) Ore-forming processes and mineral parageneses of the Jáchymov ore district. Journal of the Czech Geological Society, 48, 3-4, 157-192.

Parkhurst, D.L. and Appelo, C.A.J. (1999) User's guide to PHREEQC (Version 2) – A computer program for speciation, batch-reaction, one-dimensional transport, and inverse geochemical calculations, 312 p. US Geological Survey Water-Resources Investigations Report 99-4259,

Pearce, N.J.G., Perkins, W.T., Westgate, J.A., Gorton, M.P., Jackson, S.E, Neal C.R, and Chenery, S.P. (1997): A compilation of new and published major and trace element data for NIST SRM 610 and NIST SRM 612 glass reference materials. Geostandards Newsletter, 21, S. 115-144.

Pérez, I., Casas, I., Martín, M., and Bruno, J. (2000) The thermodynamics and kinetics of uranphane dissolution in bicarbonate test solutions. Geochimica et Cosmochimica Acta, 64,

603-608.

Pfaff, K., Romer, R.L., and Markl, G. (2009): Mineralization history of the Schwarzwald ore district: U-Pb ages of ferberite, agate, and pitchblende. European Journal of Mineralogy, 21, 817-836.

Pinto, A.J., Gonçalves, M.A., Prazeres, C., Astilleros, J.M., and Batista, M.J. (2012) Mineral replacement reactions in naturally occurring hydrated uranyl phosphates from the Tarabau deposit: Examples in the Cu–Ba uranyl phosphate system. Chemical Geology, 312-313, 18-26.

Plášil, J., Sejkora, J., Ondruš, P., Veselovský, F., Beran, P., and Goliáš, V. (2006) Supergene minerals in the Horní Slavkov uranium ore district, Czech Republic. Journal of the Czech Geological Society, 51, 1-2, 149-158.

Puchelt, H. and Emmermann, R. (1976) Bearing of rare earth patterns of apatites from igneous and metamorphic rocks. Earth and Planetary Science Letters, 31, 279-286.

Ramdohr, P. (1963) Eine subrezente Bildung von Uranpecherz aus U^{+6}-Lösungen. Jahreshefte geologisches Landesamt in Baden-Württemberg, 6, 539-542.

Schatz, R. and Otto, J. (1989) Neue Vorkommen von Pechblende bei St. Ulrich und Sulzburg im südwestlichen Schwarzwald. Jahreshefte geologisches Landesamt in Baden-Württemberg, 31, 171-182.

Schleicher, H. (1994) Collision-type granitic melts in the context of thrust tectonics and uplift

history (Triberg granite complex, Schwarzwald, Germany). Neues Jahrbuch für Mineralogie Abhandlungen, 166, 211-237.

Schwarz, M. and Henk, A. (2005) Evolution and structure of the Upper Rhine Graben: insights from three-dimensional thermomechanical modeling. International Journal of Earth Sciences, 94, 732-750.

Schwinn, G. and Markl, G. (2005) REE systematics in hydrothermal fluorite. Chemical Geology, 216, 225-248.

Simon, F.G., Biermann, V., and Peplinski, B. (2008) Uranium removal from groundwater using hydroxyapatite. Applied Geochemistry, 23, 2137-2145.

Spahiu, K. and Bruno, J. (1995) A selected thermodynamic database for REE to be used in HLNW performance assessment exercises. Technical Report 95-35, MBT Tecnologia Ambiental, Cerdanyola, Spain.

Staude, S., Bons, P.D., and Markl, G. (2009) Hydrothermal vein formation by extension-driven dewatering of the middle crust: An example from SW Germany. Earth and Planetary Science Letters, 286, 387-395.

Staude, S., Dorn, A., Pfaff, K., and Markl, G. (2010) Assemblages of Ag-Bi sulfosalts and conditions of their formation: the type locality of schapbachite ($Ag_{0.4}Pb_{0.2}Bi_{0.4}S$) and neighboring mines in the Schwarzwald ore district, southern Germany. Canadian Mineralogist, 48, 441-466.

Staude, S., Werner, W., Mordhorst, T., Wemmer, K., Jacob, D.E., and Markl, G. (2012) Multi-stage Ag-Bi-Co-Ni-U and Cu-Bi vein mineralization at Wittichen, Schwarzwald, SW Germany: geological setting, ore mineralogy, and fluid evolution. Mineralium Deposita, 47, 251-276.

Steen, H. (2007) Die Uranvorkommen des mittleren und südlichen Schwarzwaldes – Ergebnisse der Uranprospektion nach 1960. Der Erzgräber, 21 (2), 1-68.

Stille, P., Gauthier-Lafaye, F., Jensen, K.A., Salah, S., Bracke, G., Ewing, R.C., Louvat, D., and Million, D. (2003) REE mobility in groundwater proximate to the natural fission reactor at Bangombé (Gabon). Chemical Geology, 198, 289– 304.

Takahashi, Y., Shimizu, H., Usui, A., Kagi, H., and Nomura, M. (2000) Direct observation of tetravalent cerium in ferromanganese nodules and crusts by X-ray-absorption near-edge structure (XANES). Geochimica et Cosmochimica Acta, 64, 2929-2935.

Travis, C.C. and Doty, C. B. (1990) Can contaminated aquifers at Superfund sites be remediated? Environmental Science & Technology, 24, 1464-1466.

Trenfield, M.A., McDonald, S., Kovacs, K., Lesher, E.K., Pringle, J.M., Markich, S.J.,Ng, J.C., Noller, B., Brown, P.L., and van Dam, R.A. (2011) Dissolved organic carbon reduces uranium bioavailability and toxicity. 1. Characterization of an aquatic fulvic acid and its complexation with uranium[VI]. Environmental Science and Technology, 45, 3075–3081.

van Genderen, A.C.G. and van der Weijden, C.H. (1984) Predicion of Gibbs energies of formation and stability constants of some secondary uranium minerals containing the uranyl

group. Uranium, 1, 249-256.

Vochten, R. and Goeminne, A. (1984) Synthesis, crystallographic data, solubility and electrokinetic properties of meta-zeunerite, meta-kirchheimerite and nickel-uranylarsenate. Physics and Chemistry of Minerals, 11, 95-100.

Vochten, R., Piret, P., and Goeminne, A. (1981) Synthesis, crystallographic data, solubility and electrokinetic properties of copper-, nickel- and cobalt-uranylphosphate. Bulletin de Minéralogie, 104, 457-467.

Walenta, K. (1958) Die sekundären Uranmineralien des Schwarzwaldes. Jahreshefte des Geologischen Landesamtes in Baden-Württemberg, 3, 17-51.

Walenta, K. (1972): Die Sekundärmineralien der Co-Ni-Ag-Bi-U-Erzgänge im Gebiet von Wittichen im mittleren Schwarzwald. Aufschluß, 23, 279-329.

Walenta, K. (1992) Die Mineralien des Schwarzwaldes und ihre Fundstellen, 336 p. Christian Weise Verlag, München, Germany.

Wendt, I., Lenz, H., Höhndorf, A., Bültemann, H., and Bültemann, W.-D. (1979) Das Alter der Pechblende der Lagerstätte Menzenschwand, Schwarzwald. Zeitschrift der deutschen geologischen Gesellschaft, 130, 619-626.

Zuther, M. (1983) Das Uranvorkommen Müllenbach/Baden-Baden, eine epigenetisch-hydrothermale Imprägnationslagerstätte in Sedimenten des Oberkarbon (Teil I: Erzmineralbestand). Neues Jahrbuch für Mineralogie Abhandlungen, 147, 191-216.

1034 **Figure Captions**

1035

1036 Figure 1. Geological map of the Schwarzwald with major geological units (modified after
1037 Kalt et al. 2000) with sample localities. Numbers for localities refer to numbers in Table 1.

1038

1039 Figure 2. Examples of uranium minerals: a) primary magmatic uraninite I (M34/1),
1040 Menzenschwand b) primary hydrothermal uraninite II (MenzA2), Menzenschwand c)
1041 zeunerite growing on skutterudite, Wittichen d) torbernite growing over uranophane,
1042 Menzenschwand e) zeunerite growing on a granite fissure, Wittichen f) pseudomorphs of
1043 goethite after autunite group mineral, Menzenschwand g) pseudomorphs of uraninite III after
1044 ianthinite, Menzenschwand, this is a frequently observed texture described by Ramdohr
1045 (1963) h) secondary uraninite III replacing pyrite (M29/5), Menzenschwand. Photographs c)-
1046 g) are taken from Markl and Wolfsried (2011).

1047

1048 Figure 3. Ce anomalies in uraninite II samples.

1049

1050 Figure 4. La_{norm}/Gd_{norm} vs. Eu anomaly of all analyzed uraninite II samples. The
1051 analytical error is within the symbol.

1052

1053 Figure 5. PAAS normalized REE patterns of uraninite II, uranophane, uranyl phosphates
1054 and arsenates, and natural waters from Wittichen and Menzenschwand. Typical errors are
1055 valid for Menzenschwand and Wittichen samples.

1056

1057

1058 Figure 6. Overview of possible REE sources, their abundances and REE concentrations
1059 from literature (fluorite: Möller et al. 1982; Staude et al. 2012; whole rock granites:

Emmermann et al. 1975; Schleicher 1994; whole rock gneiss: Hofmann, 1989) and this work (uraninite I and II, and mine waters).

Figure 7. Gd_{norm}/Lu_{norm} vs. La_{norm}/Gd_{nomr} plot containing uraninite, secondary uranyl silicates, arsenates and phosphates, fluorite, natural waters and the whole-rock granites from Menzenschwand (a) and Wittichen (b). w=water, fl=fluorite, g=granite. Fluorite data was taken from Möller et al. (1982) and Staude et al. (2012) whole-rock granite data are from Emmermann et al. (1975) and Schleicher (1994). Typical errors are valid for Menzenschwand and Wittichen samples.

Figure 8. Distribution of complexes for La, Gd, Y and Lu during reaction with sulfides.

Figure 9. P/As ratios leading to zeunerite and torbernite formation, respectively, based on different thermodynamic data, depending on pH.

Figure 10. Stability of uranyl minerals depending on fO_2 and pH. Black line represents saturation indices equal 0. For fO_2-pH couples plotting in the grey area, the solution is oversaturated, in the white area the solution is undersaturated with respect to the mineral. Plots were calculated using PhreePlot (Kinniburgh and Cooper 2011).

Figure 11. Amount of precipitated minerals and U content in solution [mol/L] during reaction with $CuFeS_2$ and FeS_2. Reaction was calculated in 3000 steps for a higher resolution.

Figure 12. Amount of precipitated minerals and U content in solution [mol/L] during reaction with $FeAs_2$.

Fig. 1

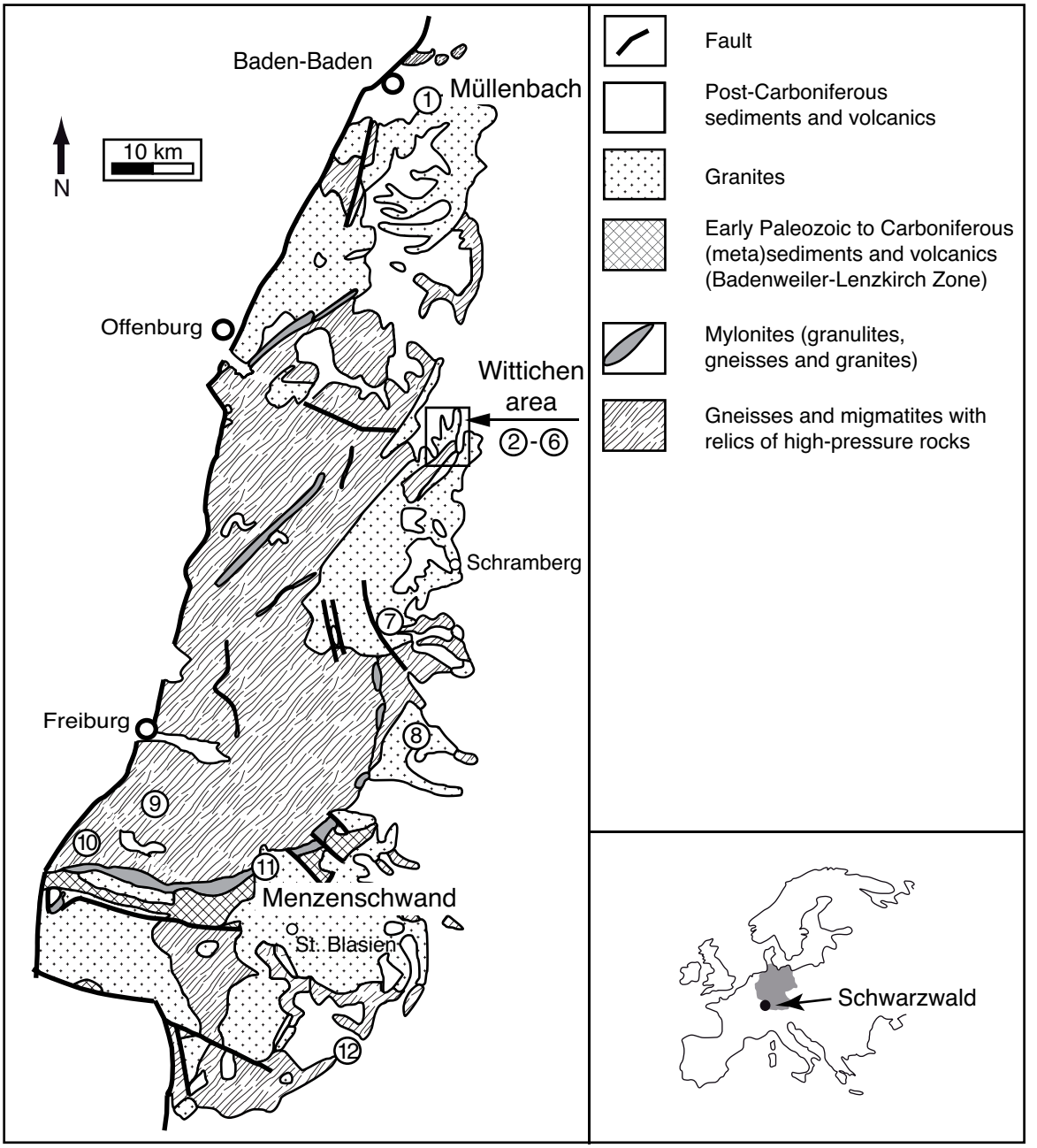
Baden-Baden
Müllenbach
1
N
10 km
Offenburg
Wittichen
area
②-⑥
Schramberg
7
Freiburg
8
9
10
11
Menzenschwand
St. Blasien
12
Fault
Post-Carboniferous
sediments and volcanics
Granites
Early Paleozoic to Carboniferous
(meta)sediments and volcanics
(Badenweiler-Lenzkirch Zone)
Mylonites (granulites,
gneisses and granites)
Gneisses and migmatites with
relics of high-pressure rocks
Schwarzwald

Fig. 2

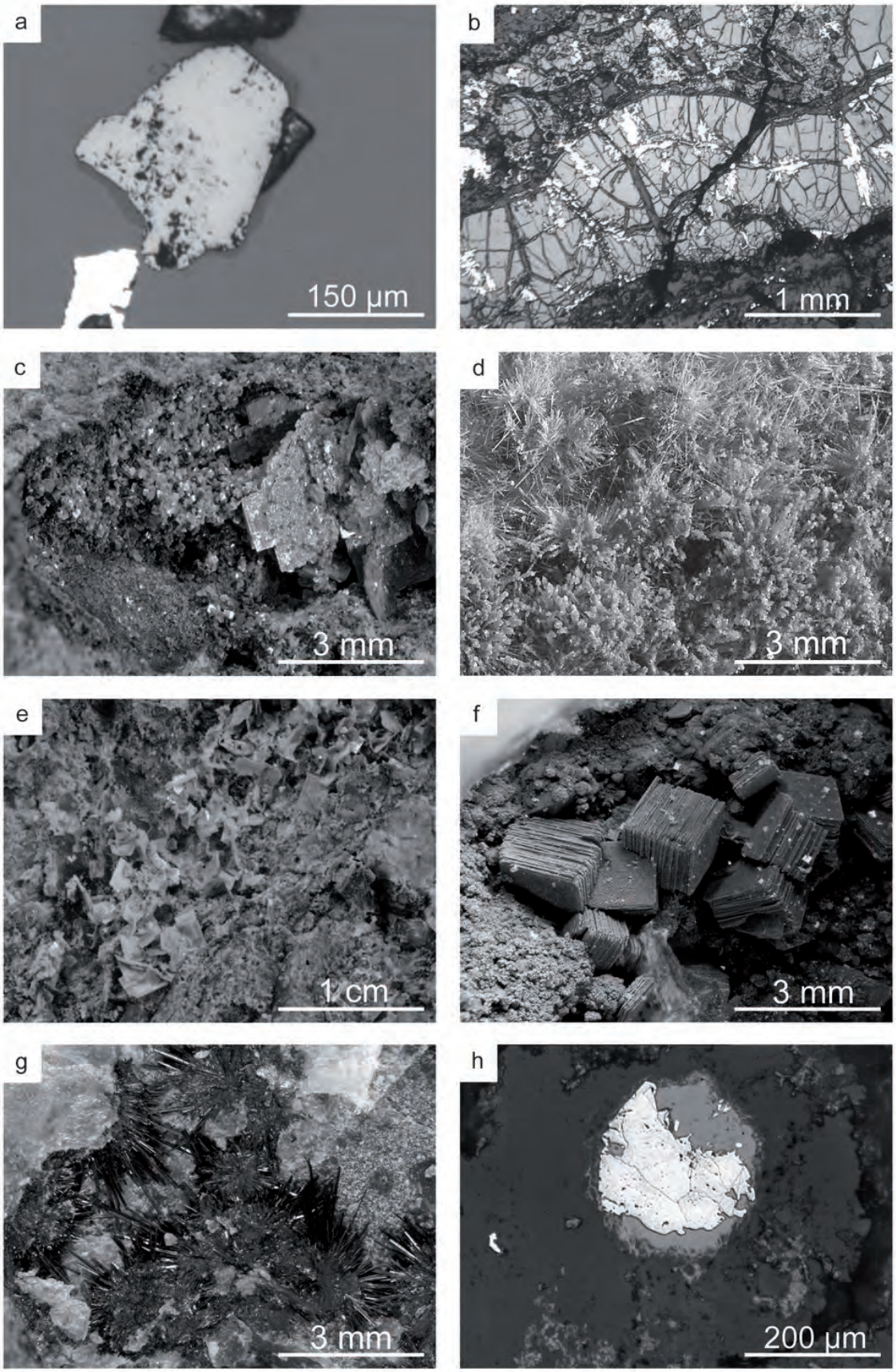

Fig. 3

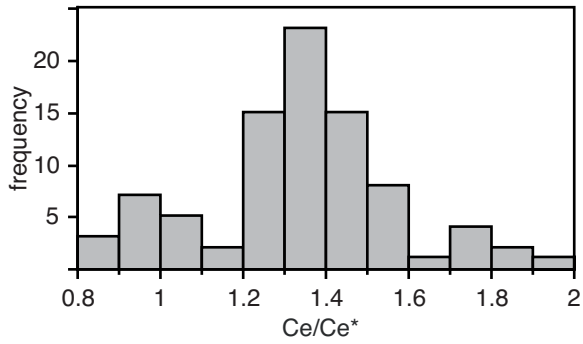

Fig. 4

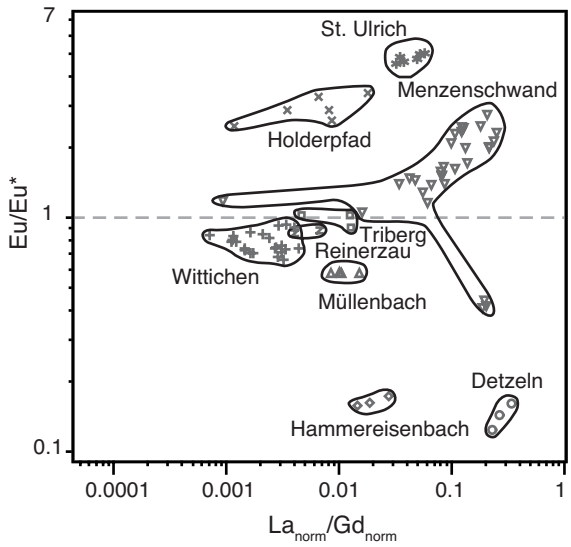
7
1
0.1
Eu/Eu*
0.0001
0.001
0.01
0.1
1
La$_{norm}$/Gd$_{norm}$
St. Ulrich
Menzenschwand
Holderpfad
Triberg
Reinerzau
Wittichen
Müllenbach
Detzeln
Hammereisenbach

Fig. 5

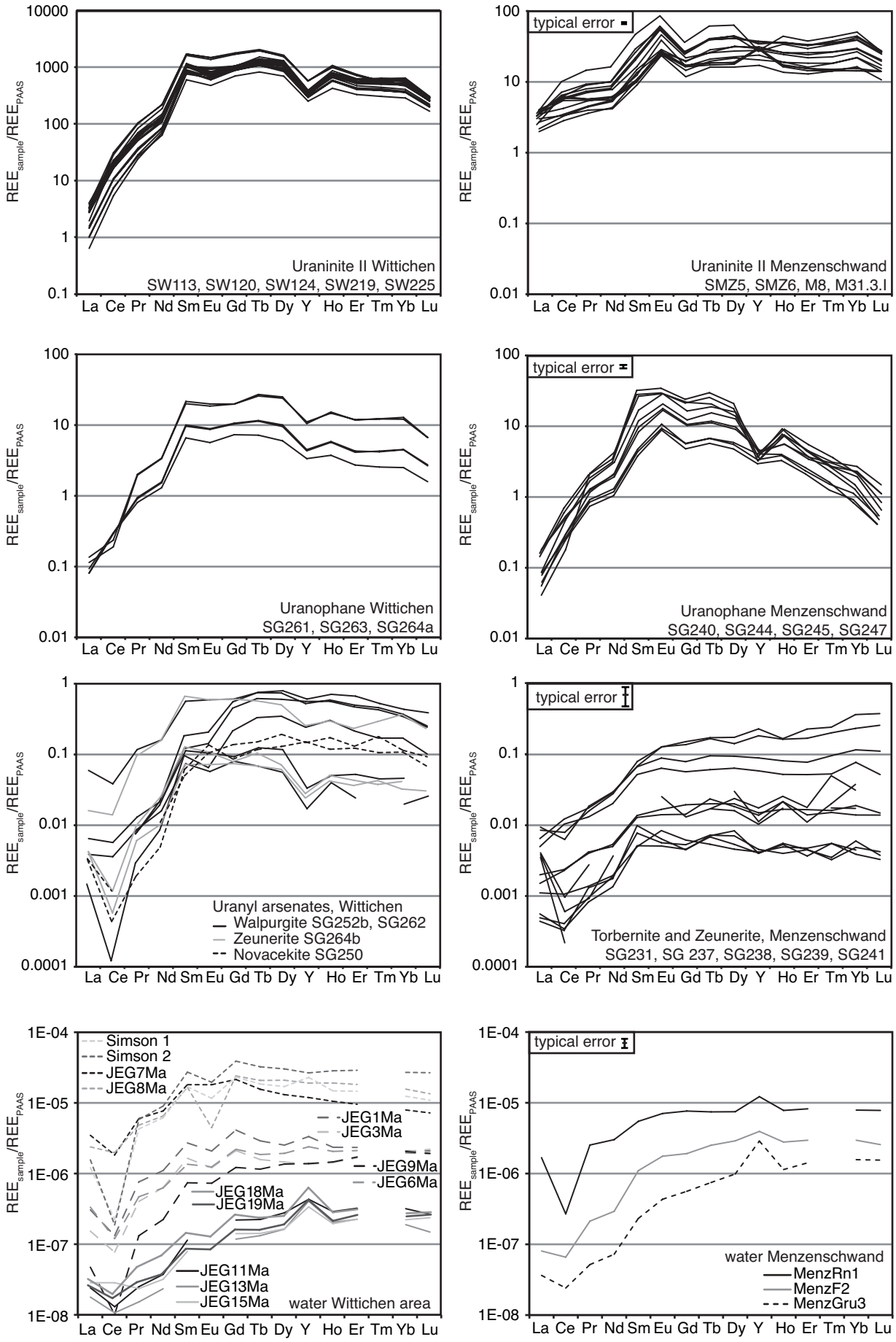
Uraninite II Wittichen
SW113, SW120, SW124, SW219, SW225
Uraninite II Menzenschwand
SMZ5, SMZ6, M8, M31.3.I
typical error
Uranophane Wittichen
SG261, SG263, SG264a
Uranophane Menzenschwand
SG240, SG244, SG245, SG247
Uranyl arsenates, Wittichen
Walpurgite SG252b, SG262
Zeunerite SG264b
Novacekite SG250
Torbernite and Zeunerite, Menzenschwand
SG231, SG 237, SG238, SG239, SG241
Simson 1
Simson 2
JEG7Ma
JEG8Ma
JEG1Ma
JEG3Ma
JEG9Ma
JEG6Ma
JEG18Ma
JEG19Ma
JEG11Ma
JEG13Ma
JEG15Ma
water Wittichen area
water Menzenschwand
MenzRn1
MenzF2
MenzGru3
REE sample/REE PAAS
La Ce Pr Nd Sm Eu Gd Tb Dy Y Ho Er Tm Yb Lu

Fig. 6

locality / source	Menzenschwand		Wittichen		
		La+Ce	La_{norm}/Yb_{norm}	La+Ce	La_{norm}/Yb_{norm}
host rock	granite:	~20 ppm	0.24-0.39	granite: 120-180 ppm	1.33-2.42
	gneiss:	~120 ppm	-		
	magmatic uraninite I:	200-300 ppm	0.003-0.005	no abundant magmatic uraninite I	
hydrothermal vein	abundant fluorite:	~10 ppm	0.03	rare fluorite:	
				fluorite I	~0.02 ppm 0.005
				fluorite II	~10 ppm 0.07
				fluorite III	~0.2 ppm 0.003
	hydrothermal uraninite II:	40-3000 ppm	0.02-0.73	hydrothermal uraninite II: 500-3000 ppm	0.002-0.01
mine waters		3-90 ppt	0.02-0.21	1-300 ppt	0.02-0.43

Fig. 7

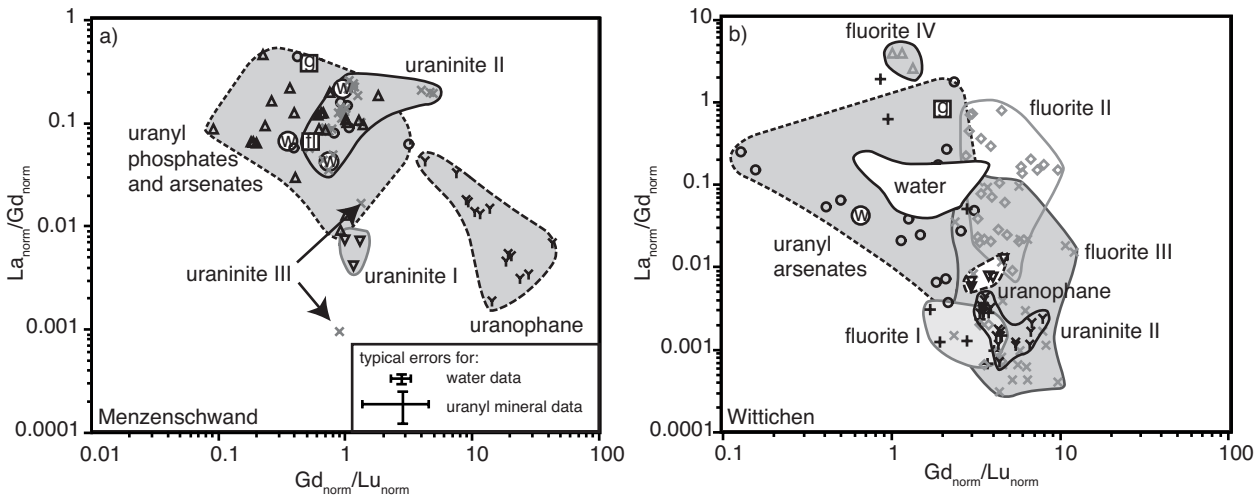
a)
uraninite II
uranyl
phosphates
and arsenates
uraninite III
uraninite I
uranophane
typical errors for:
water data
uranyl mineral data
Menzenschwand
La$_{norm}$/Gd$_{norm}$
Gd$_{norm}$/Lu$_{norm}$
b)
fluorite IV
fluorite II
water
uranyl
arsenates
fluorite III
uranophane
fluorite I
uraninite II
Wittichen

Fig. 8

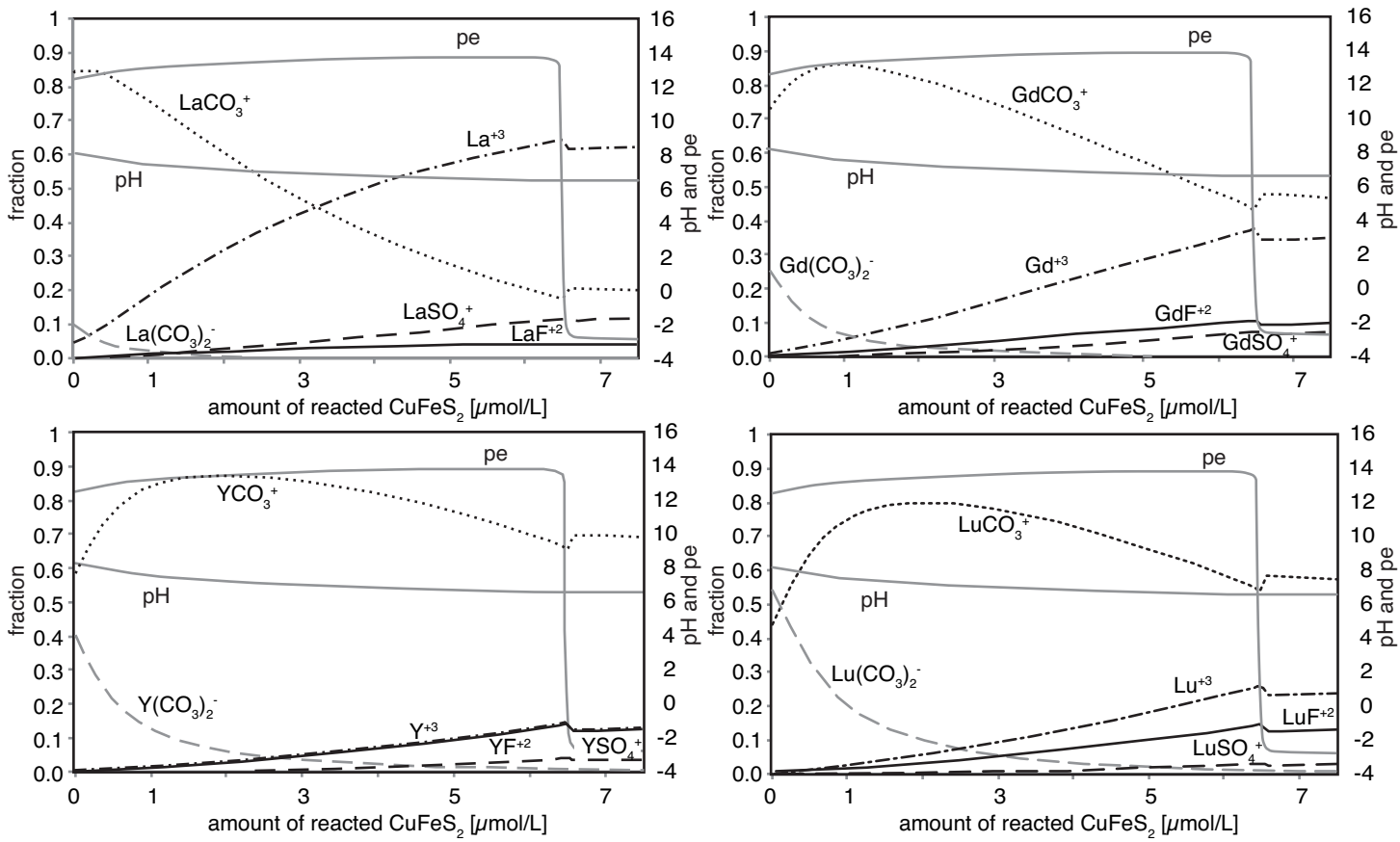
pe
LaCO3+
La+3
pH
La(CO3)2-
LaSO4+
LaF+2
fraction
pH and pe
amount of reacted CuFeS2 [μmol/L]
pe
GdCO3+
pH
Gd(CO3)2-
Gd+3
GdF+2
GdSO4+
fraction
pH and pe
amount of reacted CuFeS2 [μmol/L]
pe
YCO3+
pH
Y(CO3)2-
Y+3
YF+2
YSO4+
fraction
pH and pe
amount of reacted CuFeS2 [μmol/L]
pe
LuCO3+
pH
Lu(CO3)2-
Lu+3
LuF+2
LuSO4+
fraction
pH and pe
amount of reacted CuFeS2 [μmol/L]

Fig. 9

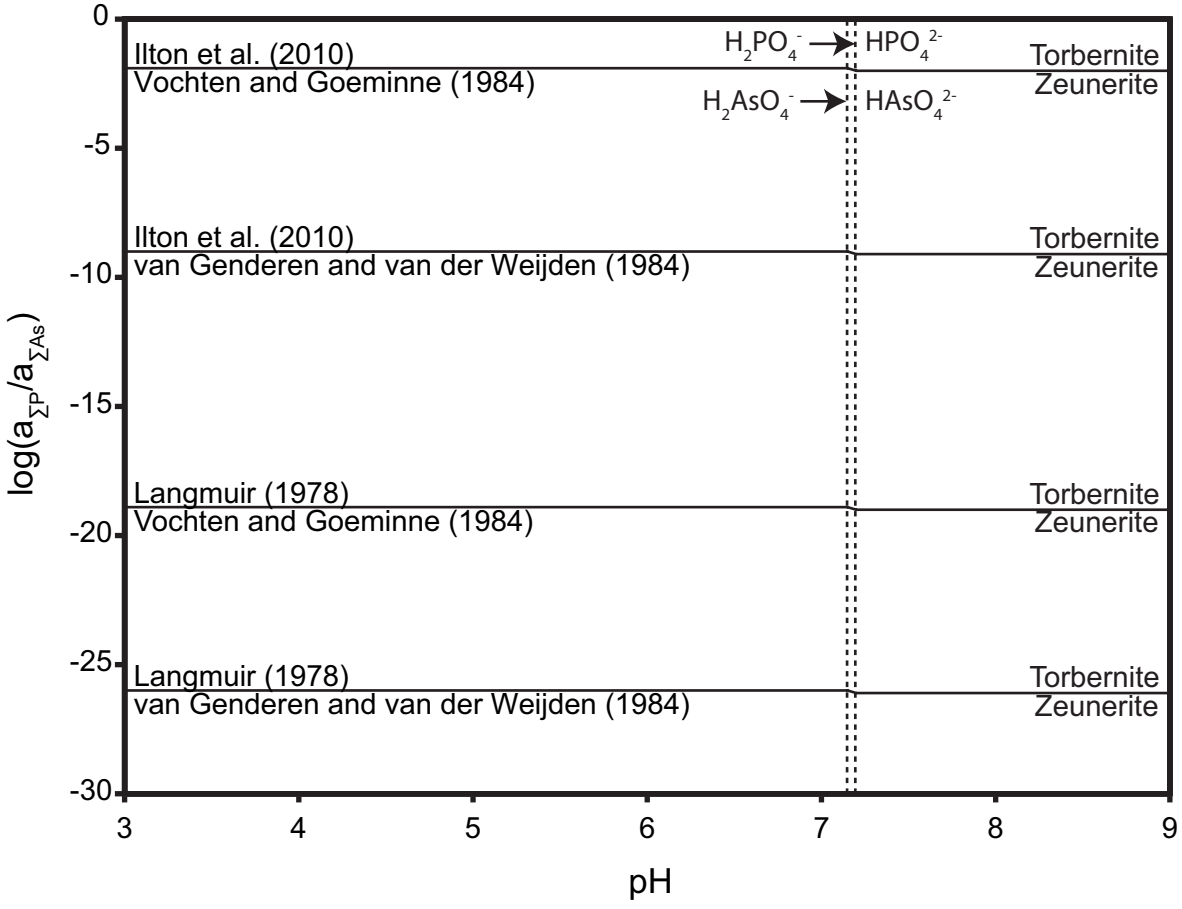
0
-5
-10
-15
-20
-25
-30
3
4
5
6
7
8
9
pH
log(a∑P/a∑As)
H2PO4- → HPO4 2-
H2AsO4- → HAsO4 2-
Ilton et al. (2010)
Vochten and Goeminne (1984)
Ilton et al. (2010)
van Genderen and van der Weijden (1984)
Langmuir (1978)
Vochten and Goeminne (1984)
Langmuir (1978)
van Genderen and van der Weijden (1984)
Torbernite
Zeunerite
Torbernite
Zeunerite
Torbernite
Zeunerite
Torbernite
Zeunerite

Fig. 10

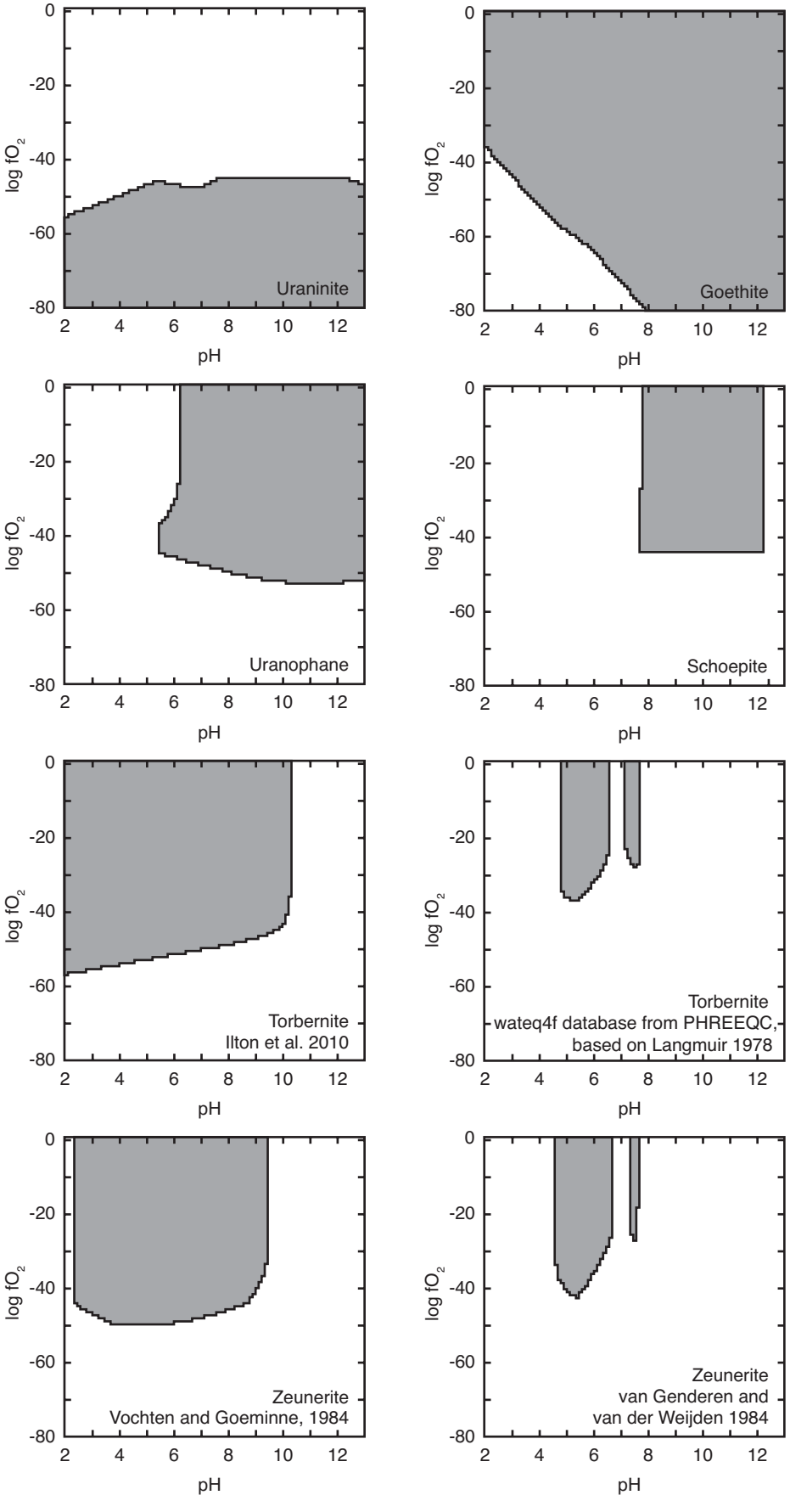
log fO2
pH
Uraninite
Goethite
Uranophane
Schoepite
Torbernite
Ilton et al. 2010
Torbernite
wateq4f database from PHREEQC,
based on Langmuir 1978
Zeunerite
Vochten and Goeminne, 1984
Zeunerite
van Genderen and
van der Weijden 1984

Fig. 11

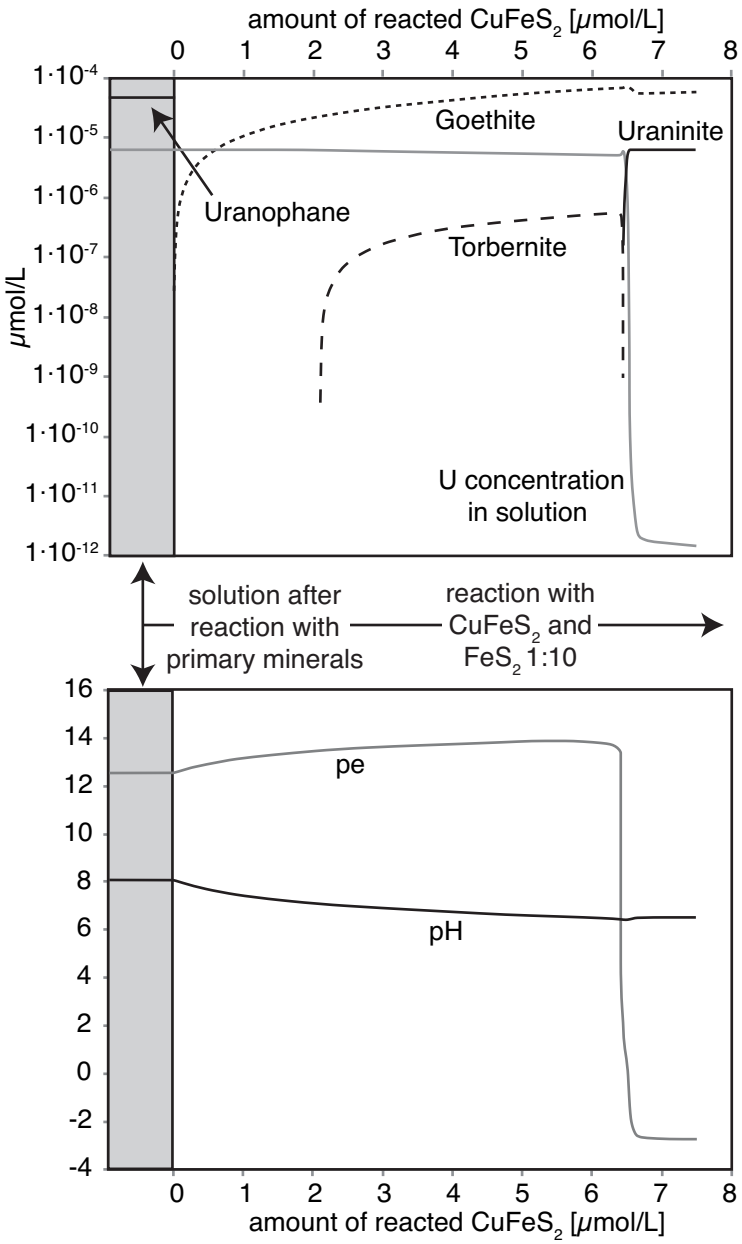
amount of reacted CuFeS2 [μmol/L]
0 1 2 3 4 5 6 7 8
1·10-4
1·10-5
1·10-6
1·10-7
1·10-8
1·10-9
1·10-10
1·10-11
1·10-12
μmol/L
Goethite
Uraninite
Uranophane
Torbernite
U concentration
in solution
solution after
reaction with
primary minerals
reaction with
CuFeS2 and
FeS2 1:10
16
14
12
10
8
6
4
2
0
-2
-4
pe
pH
0 1 2 3 4 5 6 7 8
amount of reacted CuFeS2 [μmol/L]

Fig. 12

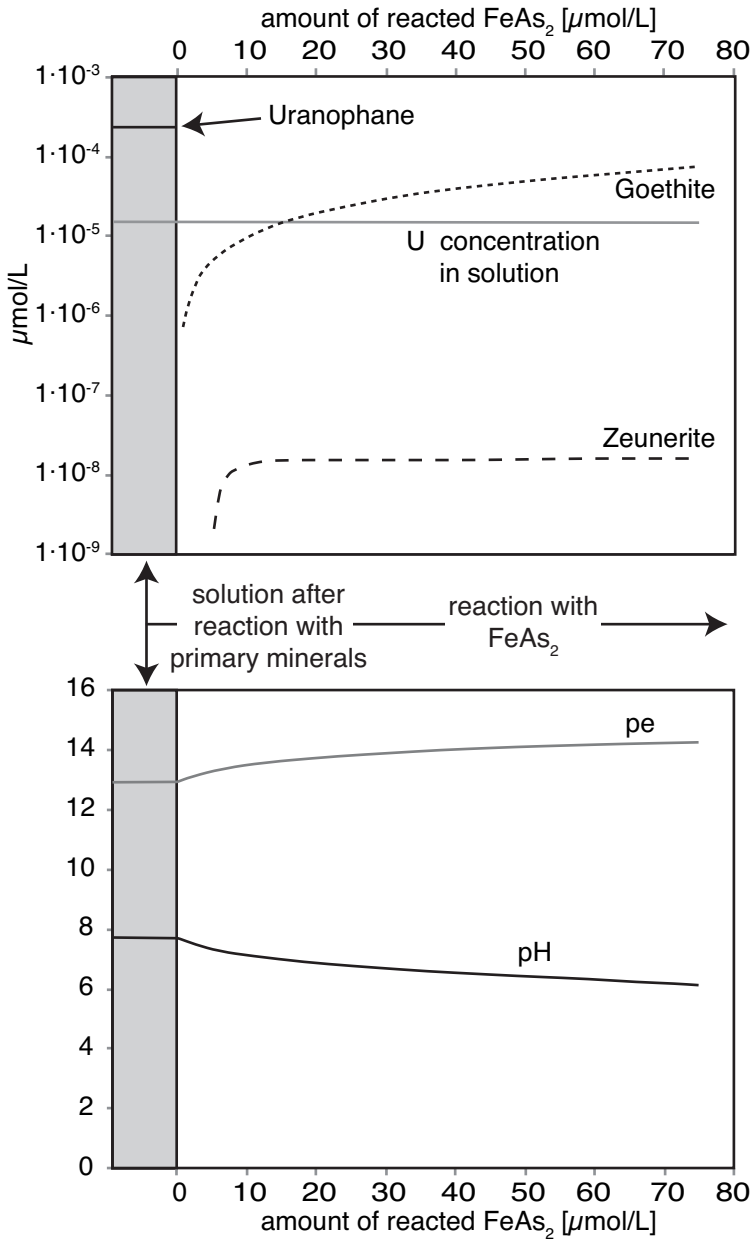
amount of reacted FeAs2 [μmol/L]
0 10 20 30 40 50 60 70 80
1·10-3
1·10-4
1·10-5
1·10-6
1·10-7
1·10-8
1·10-9
μmol/L
Uranophane
Goethite
U concentration
in solution
Zeunerite
solution after
reaction with
primary minerals
reaction with
FeAs2
16
14
12
10
8
6
4
2
0
pe
pH
0 10 20 30 40 50 60 70 80
amount of reacted FeAs2 [μmol/L]

Table 1: Localities and analyzed mineral samples

	Locality	host rock	analyzed minerals	mineral formula	samples
1	Kirchheimer Stollen, Müllenbach near Baden-Baden	carboniferous arkose and conglomerates and coal	uraninite II	UO_2	114*, SG269
2	Dreikönigstern, Reinerzau	granite	uraninite II	UO_2	SRZ22
3	Sophia, Wittichen	granite	uraninite II	UO_2	SW113, SW115, SW120, SW219, SW124, SW221, SW222, SW223
4	Schmiedestollen dump, Wittichen	granite	uraninite II	UO_2	SW225
			heinrichite	$Ba(UO_2)_2(AsO_4)_2 \cdot 10H_2O$	SG249, SG256, SG258
			nováčekite	$Mg(UO_2)_2(AsO_4)_2 \cdot 10H_2O$	SG250
			zeunerite	$Cu(UO_2)_2(AsO_4)_2 \cdot 12H_2O$	SG252a, SG253, SG259, SG260, SG264b
			walpurgite	$(BiO)_4(UO_2)(AsO_4)_2 \cdot 3H_2O$	SG252b
			uranophane	$Ca(UO_2)_2(HSiO_4)_2 \cdot 5H_2O$	SG261, SG263, SG264a
5	St. Joseph am Silberberg, Wittichen	granite	uranospinite	$Ca(UO_2)(AsO_4)_2 \cdot 10H_2O$	SG255, SG257
			walpurgite	$(BiO)_4(UO_2)(AsO_4)_2 \cdot 3H_2O$	SG262
			zeunerite	$Cu(UO_2)_2(AsO_4)_2 \cdot 12H_2O$	SG251
6	Anton, Heubachtal near Wittichen	granite	zeunerite	$Cu(UO_2)_2(AsO_4)_2 \cdot 12H_2O$	SG265, SG254
7	Nußbach near Triberg	granite	uraninite II	UO_2	STRI1, STRI2
8	Hammereisenbach	granite	uraninite II	UO_2	SHE4
9	St. Ulrich	gneiss	uraninite II	UO_2	SSTU3, SSTU4
10	Holderpfad, Sulzburg	gneiss	uraninite II	UO_2	HO3a, BO147
11	Menzenschwand	granite	uraninite I	UO_2	M34/1†
			uraninite II	UO_2	SMZ5, SMZ6, MenzA2†, M8†, M11†, M29/5†, M31/3/1†
			churchite	$REEPO_4 \cdot 2H_2O$	SG228a‡, SG229a, ‡ SG230a‡
			uranocircite	$Ba(UO_2)_2(PO_4)_2 \cdot 12H_2O$	SG228b, SG229b, SG230c, SG233b, SG234, SG235, SG236, SG267
			uranophane	$Ca(UO_2)_2(HSiO_4)_2 \cdot 5H_2O$	SG240, SG243, SG244, SG245, SG247, SG248
			beta-uranophane	$Ca(UO_2)_2(HSiO_4)_2 \cdot 5H_2O$	SG242
			cuprosklodowskite	$Cu(UO_2)_2(HSiO_4)_2 \cdot 6H_2O$	SG246
			torbernite	$Cu(UO_2)_2(PO_4)_2 \cdot 12H_2O$	SG231, SG237, SG238, SG239, SG266
			zeunerite	$Cu(UO_2)_2(AsO_4)_2 \cdot 12H_2O$	SG241
12	Detzeln near Waldshut	granite/gneiss	uraninite II	UO_2	SG232

* sample material from Hauptmann (1976)

† sample material from Hofmann (1989)

‡ results published in Göb et al.(2011)

Table 2: Water analyses of samples from Menzenschwand and the Wittichen region

Water sample	Typical error	MenzRn1	MenzF2	MenzGru3	JEG 1 Ma	JEG 3 Ma	JEG 6 Ma	JEG 7 Ma	JEG 8 Ma
Region		Menzenschwand	Menzenschwand	Menzenschwand	Wittichen area Reinerzau	Wittichen area Reinerzau	Wittichen area Reinerzau	Wittichen area Wittichen	Wittichen area Schiltach
Locality		Radon spa Menzenschwand	Fluoride spa Menzenschwand	Grube Menzenschwand/ Krunkelbach	oberer Emanuel im Hengstbach	Alte Gabe Gottes oberer Stollen	Felsenkellerstollen der Grube Dreikönigstern	Johann am Burgfelsen	Michael im Rohrbächle
Mineralization		U	U	U	Cu-Bi-Co	Cu-Bi	Co-Ni-As-U	Cu	Co-Ni-As-U
vein type		qz-fl-brt	qz-fl-brt	qz-fl-brt	fl-brt(-cb)	fl-brt	brt-fl-qz	fl-brt	brt
pH		7.3	6.6	7.1	7.7	6.6	6.8	6.3	7.1
Temperature [°C]		8.1	10.2	10.0	12.9	10.1	10.7	10.3	13.6
Conductivity [µS/cm]		47	61	70	157	30	148	40	132
TDS [mg/l]		23	30	34	77	15	73	20	64
HCO3- mg/l		36.9	32.3	41.8	105.9	20.7	97.6	24.4	23.8
Na [mg/l]	10%	2.42	2.92	3.53	1.67	1.86	3.02	2.36	10.22
K [mg/l]l	10%	0.52	1.02	0.94	1.03	0.58	1.23	0.52	2.43
Mg [mg/l]	10%	0.87	0.72	0.83	6.54	0.45	3.92	0.69	2.70
Ca [mg/l]	10%	6.59	8.51	10.16	21.21	2.65	23.97	4.59	10.30
F [mg/l]	10%	0.21	1.50	1.18	0.09	0.37	0.04	1.06	0.06
Cl [mg/l]	10%	0.95	1.00	0.89	1.20	0.54	5.87	1.09	20.74
Br [mg/l]	10%	<0.01	<0.01	<0.01	0.02	0.01	<0.01	0.01	<0.01
NO_3^- [mg/l]	10%	2.02	2.88	2.35	6.98	2.91	1.58	1.85	15.84
PO_4^{3-} [mg/l]	10%	0.02	<0.02	<0.02	0.04	0.10	0.09	0.04	<0.02
SO_4^{2-} [mg/l]	10%	2.56	4.15	4.42	3.71	2.09	3.55	5.84	7.09
La [mg/kg]	10%	6.42E-05	1.39E-06	3.07E-06	1.14E-05	5.65E-06	1.24E-05	1.32E-04	8.99E-05
Ce [mg/kg]	10%	2.14E-05	1.92E-06	5.24E-06	1.01E-05	5.90E-06	9.20E-06	1.44E-04	1.55E-04
Pr [mg/kg]	10%	2.23E-05	4.56E-07	1.88E-06	6.58E-06	3.47E-06	4.04E-06	5.27E-05	4.24E-05
Nd [mg/kg]	10%	1.02E-04	2.45E-06	9.91E-06	3.68E-05	2.10E-05	2.08E-05	2.60E-04	2.20E-04
Sm [mg/kg]	10%	3.03E-05	1.29E-06	6.11E-06	1.49E-05	8.99E-06	7.39E-06	1.01E-04	9.23E-05
Eu [mg/kg]	10%	7.63E-06	4.68E-07	1.90E-06	2.22E-06	1.28E-06	1.32E-06	1.96E-05	4.78E-06
Gd [mg/kg]	10%	3.56E-05	2.61E-06	8.92E-06	1.91E-05	9.72E-06	1.01E-05	1.00E-04	1.13E-04
Tb [mg/kg]	10%	5.76E-06	5.78E-07	1.94E-06	2.22E-06	1.20E-06	1.42E-06	1.21E-05	1.61E-05
Dy [mg/kg]	10%	3.50E-05	4.61E-06	1.36E-05	1.17E-05	6.69E-06	8.91E-06	6.12E-05	9.83E-05
Y [mg/kg]	10%	3.30E-04	7.76E-05	1.06E-04	8.93E-05	3.60E-05	6.38E-05	3.22E-04	5.17E-04
Ho [mg/kg]	10%	7.73E-06	1.13E-06	2.76E-06	2.30E-06	1.39E-06	2.01E-06	1.04E-05	1.90E-05

Er [mg/kg]	10%	2.34E-05	4.05E-06	8.43E-06	6.59E-06	4.69E-06	5.94E-06	2.72E-05	5.21E-05
Tm [mg/kg]	10%	n.a.	n.a.	n.a.	n.a.	n.a.	n.a.	n.a.	n.a.
Yb [mg/kg]	10%	2.22E-05	4.43E-06	8.34E-06	5.84E-06	5.69E-06	5.45E-06	2.23E-05	4.43E-05
Lu [mg/kg]	10%	3.38E-06	6.71E-07	1.11E-06	8.91E-07	9.42E-07	8.13E-07	3.11E-06	5.83E-06
Σ REE [mg/kg]		7.11E-04	1.04E-04	1.80E-04	2.20E-04	1.13E-04	1.54E-04	1.27E-03	1.47E-03
Th [mg/kg]	10%	4.49E-06	2.44E-06	1.00E-06	2.02E-06		4.78E-06	2.22E-05	3.19E-05
U [mg/kg]	10%	4.36E-03	5.69E-03	7.06E-02	4.55E-04	8.68E-05	5.19E-04	4.03E-04	3.29E-04
Si [mg/l]	6%	4.06E+00	4.11E+00	4.92E+00	4.46E+00	4.46E+00	3.23E+00	5.07E+00	5.68E+00
Li [mg/l]	3%	9.20E-04	3.28E-03	4.44E-03	9.28E-04	1.45E-03	4.24E-04	2.93E-03	1.30E-02
Al [mg/l]	6%	1.99E-02	4.93E-02	2.78E-02	5.11E-03	4.97E-02	5.72E-03	1.93E-01	1.71E-01
Cr [mg/l]	3%	1.34E-04	1.00E-04	9.40E-05	6.20E-05	1.00E-04	5.20E-05	6.20E-05	6.60E-05
Mn [mg/l]	3%	5.20E-04	6.88E-04	1.76E-03	1.68E-04	2.12E-04	1.17E-01	1.76E-03	3.87E-03
Fe [mg/l]	6%	5.14E-03	9.39E-03	8.13E-03	1.88E-03	9.72E-04	2.46E-02	1.40E-02	4.98E-03
Co [mg/l]	3%	<0.00001	<0.00001	3.20E-05	<0.00001	<0.00001	1.16E-04	6.40E-05	1.08E-04
Ni [mg/l]	3%	4.72E-04	2.62E-04	2.32E-04	<0.0001	<0.0001	<0.0001	4.02E-04	1.09E-03
Cu [mg/l]	3%	2.97E-03	1.16E-03	1.21E-03	<0.00015	1.03E-03	7.12E-04	3.81E-02	4.98E-04
Zn [mg/l]	3%	8.91E-03	7.23E-03	3.00E-02	2.78E-03	2.88E-03	3.47E-03	1.04E-02	3.16E-03
As [mg/l]	3%	4.32E-03	9.21E-03	1.23E-02	4.43E-03	3.53E-03	3.35E-03	2.31E-03	7.55E-03
Rb [mg/l]	3%	2.39E-03	5.83E-03	6.24E-03	5.00E-03	2.84E-03	3.53E-03	1.86E-03	1.04E-02
Sr [mg/l]	3%	2.52E-02	4.34E-02	4.93E-02	3.09E-02	1.37E-02	4.88E-02	1.60E-02	8.92E-02
Cd [mg/l]	3%	<0.000033	2.60E-05	3.60E-05	<0.000033	<0.000033	<0.000033	3.20E-05	3.00E-05
Sb [mg/l]	3%	8.80E-05	1.18E-04	5.14E-04	7.20E-05	8.20E-05	9.00E-05	1.16E-04	1.16E-04
Cs [mg/l]	3%	6.70E-04	1.56E-03	1.91E-03	2.38E-03	1.09E-02	1.13E-03	1.29E-03	5.39E-03
Ba [mg/l]	3%	2.15E-01	5.57E-01	4.41E-01	7.81E-01	1.80E-01	3.01E-01	2.26E-01	5.41E-01
Tl [mg/l]	3%	<0.00001	<0.00001	2.60E-05	<0.00001	<0.00001	<0.00001	<0.00001	<0.00001
Pb [mg/l]	3%	5.62E-04	3.40E-04	1.00E-03	<0.00001	<0.00001	<0.00001	2.86E-04	4.20E-05
Bi [mg/l]	3%	<0.00002	<0.00002	<0.00002	<0.00002	<0.00002	<0.00002	7.60E-05	<0.00002
Eu/Eu*	11%	1.09	1.20	1.21	0.62	0.65	0.72	0.92	0.22
Ce/Ce*	11%	0.13	0.56	0.50	0.27	0.31	0.30	0.40	0.58
Y/Ho	14%	42.67	68.74	38.56	38.76	25.88	31.75	30.82	27.24

n.a.=not analyzed

Table 2 (continued)

Water sample	Typical error	JEG 9 Ma	JEG 11 Ma	JEG 13 Ma	JEG 15 Ma	JEG 18 Ma	JEG 19 Ma	Simson1	Simson2
Region		Wittichen area	Wittichen area	Wittichen area	Wittichen area	Wittichen area	Wittichen area	Wittichen area	Wittichen area
		Schiltach	Wittichen	Wittichen	Wittichen	Reinerzau	Reinerzau	Wittichen	Wittichen
Locality		Hilfe Gottes	Güte Gottes im Zundelgraben	Johann Georg im Böckelsbach	Anton im Heubach	Flussspatgrube Reinerzau	Herzog Friedrich	Simson im Böckelsbach	Simson im Böckelsbach
Mineralization		Cu-Bi-Co-U	Co-Ni-As-U	Co-Ni-As-U	Co-Ni-As-U	Cu	Co-Ni-As-U	Co-Ni-As-U	Co-Ni-As-U
vein type		brt-qz	brt	brt	brt	fl-brt	brt	brt	brt
pH		6.9	7.2	7.7	6.8	7.5	8.3	7.3	7.1
Temperature [°C]		11.7	12.0	8.8	8.7	10.3	8.8	9.8	9.0
Conductivity [µS/cm]		174.6	371	208	147	174.9	302	69	53
TDS [mg/l]		85	180	101	72	85	148	34	26
HCO3- mg/l		91.8	258.1	163.2	113.8	114.4	223.9	38.1	28.4
Na [mg/l]	10%	4.51	5.09	3.14	2.07	4.40	4.62	1.69	1.63
K [mg/l]l	10%	1.16	9.55	1.83	1.88	1.15	2.12	1.14	1.18
Mg [mg/l]	10%	8.35	22.45	8.01	7.21	6.96	18.58	2.73	1.98
Ca [mg/l]	10%	19.64	39.26	31.96	19.97	24.46	38.53	8.46	5.44
F [mg/l]	10%	0.17	0.05	0.11	0.05	1.49	0.54	0.06	0.06
Cl [mg/l]	10%	6.82	9.99	1.53	1.46	1.68	1.63	1.07	1.06
Br [mg/l]	10%	<0.01	0.02	<0.01	<0.01	<0.01	<0.01	<0.01	<0.01
NO_3^- [mg/l]	10%	12.59	10.99	1.40	2.45	2.53	1.50	5.23	5.48
PO_4^{3-} [mg/l]	10%	0.10	0.11	0.02	<0.02	0.02	<0.02	0.09	0.12
SO_4^{2-} [mg/l]	10%	13.43	7.26	4.58	6.76	5.39	7.71	5.09	5.53
La [mg/kg]	10%	1.73E-06	8.79E-07	6.48E-07	1.04E-06	1.32E-06	1.08E-06	4.56E-05	5.87E-05
Ce [mg/kg]	10%	7.62E-07	9.86E-07	8.07E-07	2.17E-06	1.69E-06	1.48E-06	1.73E-05	1.44E-05
Pr [mg/kg]	10%	1.13E-06	2.11E-07	1.28E-07	1.98E-07	4.48E-07	2.74E-07	3.75E-05	5.11E-05
Nd [mg/kg]	10%	7.34E-06	1.21E-06	7.57E-07	1.03E-06	2.49E-06	1.35E-06	2.08E-04	3.04E-04
Sm [mg/kg]	10%	4.02E-06	6.12E-07		4.23E-07	8.40E-07	5.05E-07	9.38E-05	1.52E-04
Eu [mg/kg]	10%	7.70E-07				1.45E-07	9.62E-08	1.25E-05	2.12E-05
Gd [mg/kg]	10%	5.59E-06	9.94E-07	5.31E-07	6.35E-07	1.27E-06	7.85E-07	1.09E-04	1.83E-04
Tb [mg/kg]	10%	8.77E-07	1.68E-07	9.87E-08	1.06E-07	1.90E-07	1.29E-07	1.43E-05	2.53E-05
Dy [mg/kg]	10%	6.27E-06	1.26E-06	7.39E-07	7.48E-07	1.22E-06	9.29E-07	7.99E-05	1.43E-04
Y [mg/kg]	10%	3.67E-05	1.14E-05	1.07E-05	8.86E-06	1.75E-05	1.17E-05	6.21E-04	7.22E-04
Ho [mg/kg]	10%	1.42E-06	2.79E-07	1.96E-07	1.88E-07	2.91E-07	2.21E-07	1.47E-05	2.84E-05

Er [mg/kg]	10%	4.82E-06	8.95E-07	6.23E-07	6.25E-07	9.20E-07	7.68E-07	4.17E-05	8.30E-05
Tm [mg/kg]	10%	n.a.	n.a.	n.a.	n.a.	n.a.	n.a.	n.a.	n.a.
Yb [mg/kg]	10%	5.69E-06	8.73E-07	5.17E-07	6.08E-07	8.00E-07	7.25E-07	3.50E-05	7.67E-05
Lu [mg/kg]	10%	8.25E-07	1.12E-07	6.22E-08	9.96E-08	1.27E-07	1.18E-07	4.72E-06	1.16E-05
Σ REE [mg/kg]		7.80E-05	1.99E-05	1.58E-05	1.67E-05	2.92E-05	2.02E-05	1.33E-03	1.88E-03
Th [mg/kg]	10%						3.13E-06		
U [mg/kg]	10%	1.14E-03	3.05E-02	3.42E-02	3.68E-03	6.88E-03	3.32E-02	8.75E-04	
Si [mg/l]	5%	6.35E+00	3.43E+00	5.54E+00	4.21E+00	5.22E+00	4.53E+00	4.34E+00	4.27E+00
Li [mg/l]	3%	4.93E-03	7.12E-03	8.50E-03	4.04E-03	1.20E-02	1.71E-02	6.41E-03	3.36E-03
Al [mg/l]	3%	8.02E-04	8.86E-04	<0.0003	8.50E-04	1.96E-03	1.71E-03	2.89E-02	2.42E-02
Cr [mg/l]	3%	7.00E-05	8.80E-05	5.60E-05	9.40E-05	5.40E-05	5.80E-05	1.50E-04	1.68E-04
Mn [mg/l]	3%	<0.00003	1.44E-04	9.20E-05	4.06E-04	7.56E-04	1.39E-03	<0.00003	<0.00003
Fe [mg/l]	3%	<0.0002	9.20E-04	<0.0002	8.68E-04	1.75E-03	2.09E-03	8.67E-03	3.68E-03
Co [mg/l]	3%	4.60E-05	5.40E-05	7.52E-04	4.60E-05	<0.00001	5.08E-04	<0.00001	<0.00001
Ni [mg/l]	3%	<0.0001	<0.0001	3.97E-03	4.38E-04	<0.0001	6.76E-04	1.83E-03	1.53E-03
Cu [mg/l]	3%	<0.00015	<0.00015	<0.00015	<0.00015	3.56E-04	5.96E-04	<0.00015	<0.00015
Zn [mg/l]	3%	3.35E-03	3.81E-03	3.53E-03	3.39E-03	5.31E-03	5.12E-03	3.63E-03	3.18E-03
As [mg/l]	3%	1.13E-02	4.73E-02	3.31E-01	1.87E-02	2.59E-02	2.50E-01	5.35E-03	2.54E-03
Rb [mg/l]	3%	6.32E-03	3.50E-02	1.15E-02	7.95E-03	5.81E-03	9.39E-03	4.82E-03	4.04E-03
Sr [mg/l]	3%	2.25E-02	3.83E-01	6.00E-01	9.32E-02	8.26E-02	5.91E-01	2.02E-02	1.59E-02
Cd [mg/l]	3%	<0.000033	<0.000033	1.40E-05	<0.000033	<0.000033	8.00E-06	<0.000033	<0.000033
Sb [mg/l]	3%	3.00E-05	4.80E-04	4.62E-04	5.60E-05	2.82E-04	2.50E-04	<0.00001	<0.00001
Cs [mg/l]	3%	2.95E-03	7.79E-03	6.49E-03	7.94E-03	1.04E-02	3.44E-03	7.34E-03	8.24E-03
Ba [mg/l]	3%	3.97E-01	4.51E-01	3.40E-01	4.66E-01	4.14E-01	2.43E-01	2.01E-01	2.11E-01
Tl [mg/l]	3%	<0.00001	<0.00001	<0.00001	<0.00001	<0.00001	<0.00001	<0.00001	<0.00001
Pb [mg/l]	3%	<0.00001	2.40E-05	5.80E-05	3.00E-05	<0.00001	6.80E-05	5.20E-04	<0.00001
Bi [mg/l]	3%	<0.00002	<0.00002	<0.00002	<0.00002	<0.00002	<0.00002	<0.00002	<0.00002
Eu/Eu*	11%	0.77				0.66	0.72	0.58	0.60
Ce/Ce*	11%	0.13	0.53	0.65	1.10	0.51	0.63	0.10	0.06
Y/Ho	14%	25.81	40.74	54.65	47.22	60.11	53.18	42.30	25.46

Table 3: Selected REE concentrations of uraninite in ppm

Sample	Typical error	SG269	SW113b	SW124	SW225b	STRI2	SHE4a	SSTU3	Ho3a	M34/1	SMZ5	M8	Menz A2	M31.3.I	M29/5
Locality		Müllenbach	Wittichen, Sophia	Wittichen, Sophia	Wittichen, Schmiede-stollen dump	Triberg	Hammer-eisenbach	St. Ulrich	Holderpfad	Menzen-schwand	Menzen-schwand	Menzen-schwand	Menzen-schwand	Menzen-schwand	Menzen-schwand
Mineral		hydrother. uraninite II	hydrother. uraninite II	hydrother. uraninite II	hydrother. uraninite II	hydrother. uraninite II	hydrother. uraninite II	hydrother. uraninite II	hydrother. uraninite II	mag. Uraninite I	hydrother. uraninite II	hydrother. uraninite II	hydrother. uraninite II	hydrother. uraninite II	uraninite III
La	4%	104	24.7	145	109	9.81	177	477	75.8	26.9	114	151	332	120	14.9
Ce	4%	362	437	2507	1327	58.9	1655	3356	1037	252	265	463	2709	482	70.9
Pr	4%	90.6	214	929	449	19.1	521	752	495	67.8	34.9	49.8	382	67.1	13.2
Nd	4%	688	2404	7436	3687	177	2987	3902	5628	452	140	197	1388	285	82
Sm	4%	659	4519	9587	5585	157	1056	1878	6197	428	49.8	57.5	241	116	52
Eu	4%	90.1	780	1617	998	23.2	33.2	1815	3614	1.56	25.5	29.7	19.7	60.2	16.9
Gd	4%	823	4250	8404	4719	93.4	782	1666	7879	453	55	77.3	213	118	112
Tb	4%	130	873	1601	1056	11.4	115	291	1426	151	12.5	14.1	25.9	31.5	26.2
Dy	4%	524	4279	7680	5677	56.7	584	1540	8822	988	75.8	88	125	199	171
Y	4%	1653	8468	15706	9835	190	4544	5602	52318	2676	463	793	1073	1016	747
Ho	4%	66.3	588	1076	787	7.64	99.5	245	1680	147	13.5	16.8	19.9	37	30.7
Er	4%	116	1241	2089	1766	17.5	237	555	4228	376	36.8	43.6	43.4	96.6	76.1
Tm	4%	12.8	170	236	232	2.03	31.4	69.9	532	59.2	5.76	6.05	5.34	15.8	10.9
Yb	4%	67.9	1072	1389	1692	15.1	193	442	3498	432	46.2	43.4	33.5	129	74.8
Lu	4%	6.59	90.5	114	125	1.4	23.4	43	432	41.3	4.62	6.1	3.95	12.1	7.72
Eu/Eu*	5%	0.58	0.84	0.85	0.92	0.90	0.17	4.83	2.44	0.02	2.29	2.10	0.41	2.42	1.04
Ce/Ce*	5%	0.86	1.39	1.58	1.38	0.99	1.26	1.29	1.24	1.36	0.97	1.23	1.76	1.24	1.17
Y/Ho	6%	24.93	14.40	14.60	12.50	24.87	45.67	22.87	31.14	18.20	34.30	47.20	53.92	27.46	24.33

Table 4: Selected REE concentrations of secondary (supergene) uranyl minerals in ppm

Sample	Typical error	SG261	SG263	SG264b	SG265	SG249	SG258	SG255	SG250	SG262	SG246	SG247	SG237	SG228b	SG267
Locality		Wittichen, Schmiede-stollen dump	Wittichen, Schmiede-stollen dump	Wittichen, Schmiede-stollen dump	Anton im Heubachtal	Wittichen, Schmiede-stollen dump	Wittichen, Schmiede-stollen dump	Wittichen, St. Joseph am Silberberg	Wittichen, Schmiede-stollen dump	Wittichen, St. Joseph am Silberberg	Menzen-schwand	Menzen-schwand	Menzen-schwand	Menzen-schwand	Menzen-schwand
Mineral		uranophane	uranophane	zeunerite	zeunerite	heinrichite	heinrichite	uranospinit	nováčekite	walpurgite	cuprosklo-dowskite	uranophane	torbernite	uranocircite	uranocircite
La	5%	3.15	3.65	0.162	0.15	0.182	0.252	0.232	0.127	0.057	6.06	5.17	0.167	15.9	0.28
Ce	5%	24.3	24.3	0.093	0.413	0.092	0.107	0.032	0.035	0.01	22.6	48.5	0.258	8.37	0.328
Pr	5%	8.3	7.35	0.088	0.28	0.058	0.038	0.039	0.017	0.026	5.62	18.1	0.114	11.8	0.055
Nd	5%	53.5	45.6	0.845	3.55	0.549	0.262	<0.113	0.169	0.288	37.6	159	0.589	56	0.148
Sm	5%	55.6	38	0.692	5.04	0.642	0.241	<0.095	0.347	0.524	39.2	173	0.538	22.5	0.109
Eu	5%	9.74	6.34	0.114	1.00	-	-	0.291	0.151	0.069	6.92	69.7	0.068	-	-
Gd	5%	50.3	35.4	0.362	8.97	1.07	0.578	0.207	0.409	0.974	17.5	203	0.206	15.7	0.158
Tb	5%	9.15	5.79	0.079	1.45	0.258	0.081	0.029	0.093	0.248	3.55	38.2	0.054	3.42	0.038
Dy	5%	46.4	29.1	0.327	7.36	1.19	0.426	0.221	0.621	1.57	16.7	184	0.383	19.1	0.188
Y	5%	121	93.9	0.745	51.1	8.95	3.23	3.23	4.15	6.34	18	347	1.07	90.1	2.26
Ho	5%	5.87	3.84	0.049	1.58	0.207	0.086	0.033	0.12	0.291	2.03	23	0.054	3	0.031
Er	5%	12.2	8.04	0.121	3.75	0.666	0.283	0.116	0.358	0.594	4.7	36.7	0.127	7.79	0.107
Tm	5%	1.8	1.07	0.015	0.422	0.099	0.056	<0.012	0.044	0.067	0.681	2.97	0.013	1.37	0.016
Yb	5%	13.2	7.32	0.115	2.58	0.849	0.802	<0.077	0.311	0.467	4.73	11.7	0.135	15.4	0.311
Lu	5%	1.23	0.709	<0.006	0.167	0.087	0.131	<0.021	0.03	0.043	0.38	0.775	0.018	2.14	0.039
Eu/Eu*	6%	0.87	0.81	1.07	0.70				1.89	0.45	1.24	1.75	0.96		
Ce/Ce*	6%	1.10	1.08	0.18	0.46	0.21	0.25	0.08	0.17	0.06	0.89	1.16	0.43	0.14	0.61
Y/Ho	7%	20.61	24.45	15.20	32.34	43.24	37.56	97.88	34.58	21.79	8.87	15.09	19.81	30.03	72.90

Table 5: Comparison of log K values for uranophane, torbernite and zeunerite from literature

	reaction	log K	reference
Uranophane	$Ca(H_3O)_2(UO_2)_2(SiO_4)_2{\cdot}3H_2O + 6\ H^+ = Ca^{2+} + 2\ UO_2^{2+} + 2\ H_4SiO_4 + 5\ H_2O$	11.7	Pérez et al., 2000
	$Ca(H_3O)_2(UO_2)_2(SiO_4)_2{\cdot}3H_2O + 6\ H^+ = Ca^{2+} + 2\ UO_2^{2+} + 2\ SiO_2 + 9\ H_2O$	9.42	Nguyen et al., 1992
	$Ca(UO_2)_2(SiO_3)_2(OH)_2 + 6\ H^+ = Ca^{2+} + 2\ UO_2^{2+} + 2\ H_4SiO_4$	11.7	wateq4f original database, Ball and Nordstrom, 2001, based on Pérez et al., 2000
	$Ca(UO_2)_2(SiO_3)_2(OH)_2 + 6\ H^+ = Ca^{2+} + 2\ UO_2^{2+} + 2\ H_4SiO_4$	17.5	wateq4f database in PHREEQC
	$Ca(UO_2)_2(SiO_3)_2(OH)_2 + 6\ H^+ = Ca^{2+} + 2\ UO_2^{2+} + 2\ SiO_2 + 4\ H_2O$	17.3	llnl database in PHREEQC
Torbernite	$Cu(UO_2)_2(PO_4)_2{\cdot}8H_2O + 2H^+ = Cu^{2+} + 2\ UO_2^{2+} + 2HPO_4^{2-} + 8\ H_2O$	-28	Ilton et al., 2010
	$Cu(UO_2)_2(PO_4)_2{\cdot}8H_2O + 2H^+ = Cu^{2+} + 2\ UO_2^{2+} + 2H_2PO_4^{-} + 8\ H_2O$	-12.8	Vochten et al., 1981
	$Cu(UO_2)_2(PO_4)_2{\cdot}8H_2O + 4H^+ = Cu^{2+} + 2\ UO_2^{2+} + 2HPO_4^{2-} + 8\ H_2O$	-27.2	recalculated after Vochten et al., 1981
	$Cu(UO_2)_2(PO_4)_2{\cdot}nH_2O + 2H^+ = Cu^{2+} + 2\ UO_2^{2+} + 2HPO_4^{2-} + n\ H_2O$	-30	Magalhães and Pedrosa de Jesus, 1985
	$Cu(UO_2)_2(PO_4)_2 = Cu^{2+} + 2\ UO_2^{2+} + 2PO_4^{3-}$	-45.3	wateq4f database in PHREEQC, based on Langmuir, 1978
	$Cu(UO_2)_2(PO_4)_2 + 2H^+ = Cu^{2+} + 2\ UO_2^{2+} + 2HPO_4^{2-}$	-20.6	recalculated after wateq4f database in PHREEQC, based on Langmuir, 1978
	$Cu(UO_2)_2(PO_4)_2 + 2H^+ = Cu^{2+} + 2\ UO_2^{2+} + 2HPO_4^{2-}$	-20.3	llnl database in PHREEQC
Zeunerite	$Cu(UO_2)_2(AsO_4)_2{\cdot}nH_2O = Cu^{2+} + 2\ UO_2^{2+} + 2AsO_4^{3-} + n\ H_2O$	-49.2	Vochten et al., 1984
	$Cu(UO_2)_2(AsO_4)_2 = Cu^{2+} + 2\ UO_2^{2+} + 2AsO_4^{3-}$	-42.2	van Genderen and van der Weijden, 1984, based on estimation, reaction not given in original publication